



Mapping update and analysis of the evolution of non-built (green) spaces in the Brussels Capital Region

ActuaEvol/09

- Part I : Mapping of non-built (green) spaces based on recent high resolution remote sensing data
- Part II : Analysis of the evolution of non-built (green) spaces in and around the Brussels Capital Region over the last decades.

Final report

Tim Van de Voorde
Frank Canters
Jonathan Cheung-Wai Chan

December 2010

Cartography and GIS Research Group
Department of Geography
Vrije Universiteit Brussel
Pleinlaan 2, 1050 Brussel



SUMMARY

The Ordinance on the Conservation of Nature requires the development of a “Nature Plan”, which provides objective guidance for nature policy on the state of the environment in the Brussels Capital Region (BCR). This requires knowledge on the distribution, typology and quality of urban green spaces and their changes through time. This report presents the results of the project “*Actualisatie van de kartering en analyse van de evolutie van de onbebouwde (groene) gebieden in het Brussels Hoofdstedelijk Gewest (ActuaEvol/09)*”. The goal of this project was to investigate the potential of high and medium resolution multispectral remote sensing for mapping urban green, for analysing the spatial pattern of urban green (fragmentation/isolation of vegetation patches), and for monitoring changes in green coverage through time. The project consists of three parts; the first two parts are discussed in this document:

- Part I : Mapping of non-built (green) spaces based on recent high resolution remote sensing data.
- Part II : Analysis of the evolution of non-built (green) spaces in and around the Brussels Capital Region over the last decades.
- Part III: Discussion of 10 typical cases of urbanisation, fragmentation and quality evolution of non-built (green) spaces (1950-).

In part I, high resolution remote sensing data of May/June 2008 was used to map the spatial distribution of urban green within the administrative bounds of the BCR. Area calculations based on the developed maps indicated that 54% of the BCR is covered by vegetation, most of which is dense vegetation (44.25% of the total area). Despite this high average, most green areas are located in the periphery, especially in the eastern and south-eastern parts of the city. A map of vegetation density calculated at the level of street surfaces highlighted the presence of green along major axes connecting the centre to the periphery and along axes aligned with the concentric pattern of urban development. The spatial pattern of open and dense vegetation patches was described by spatial metrics quantifying fragmentation and isolation. Metrics were calculated for the BCR as a whole, as well as for 4 biological sub-regions located NW, NE, SW (rural influence) and SE (forest influence) of the city centre. Different minimum mapping units were applied, and their effect on the metrics illustrated the scale dependency of the spatial pattern. Open vegetation is highly fragmented as it consists of a large number of relatively small patches. The degree of fragmentation was found to be somewhat smaller in the NW due to the presence of relatively large agricultural parcels. Dense vegetation is characterised by larger average patch sizes and is therefore less fragmented, but the skewed patch size distribution is nevertheless dominated by small patches. Analysis of patch isolation with Euclidean nearest neighbour distance (*ENN*) and proximity index (*PROX*) pointed to a tendency for clustering of patches. Both metrics indicated that dense vegetation is much more clustered than open vegetation, except in the NW region where *PROX* values for open and dense vegetation were similar. In the SE region, the metrics confirmed a strong presence and spatial clustering of dense vegetation in and around the Sonian Forest.

In part II, the temporal evolution of urban green in and around the BCR was mapped from 4 medium resolution satellite images of 1978, 1989, 2001 and 2008. First, land-cover maps were derived for each image by assigning the pixels to one of four classes: open vegetation, dense vegetation, urban area and water. Accuracy assessment carried out for the 2008 image pointed to a relatively high overall accuracy (87% correctly classified). Some very small dense vegetation patches within the dense urbanised area were not detected because of the sensor’s limited spatial resolution, but this did not influence the analysis with spatial metrics as these patches fell below the minimum mapping threshold. During the time-period covered by the images, 4503ha of land became urbanised at the expense of both open and dense vegetation. This corresponds to a relative increase in urban land from 45.8% to 55.2% within the area covered by the BCR and a buffer of 5km surrounding it. Given the relatively coarse spatial resolution of the images, sub-pixel vegetation and sealed surface proportions were also determined to take into account that the pixels may cover multiple land-cover types, which leads to wrong area estimations. The decline in vegetation cover as calculated from the proportion maps proved more moderate with 1903ha between 1989 and 2008, but hides the fact that urbanisation often consists of low density residential development which includes vegetation in private gardens. Open vegetation became more fragmented with time and small dense vegetation patches disappeared, often because their area fell below the minimum mapping units. Patches of both open and dense vegetation demonstrated a tendency for spatial clustering, which was slightly more pronounced for open vegetation. A large part of the changes in the landscape pattern described by the metrics could be explained by increasing fragmentation, but differences in image resolution also played a part as patches frequently became split up due to a better detection of line infrastructure in images with a higher spatial resolution.

PART I: MAPPING OF NON-BUILT (GREEN) SPACES BASED ON RECENT HIGH RESOLUTION REMOTE SENSING DATA

Objectives

The first phase of the project focuses on the use of high resolution satellite data (Quickbird) for:

- 1) estimating the area covered by urban green and mapping of its spatial distribution;
- 2) analysing the pattern of urban green (fragmentation, isolation) using spatial metrics;
- 3) documenting major changes in land cover within the mapping units of the “Biologische waarderingskaart” (BWK).

The description of the tasks to be carried within this phase of the project was agreed upon during the kick-off meeting of the project organized on 19/2/2010 and is documented in the minutes of the meeting. While the first phase of the project was carried out, two follow-up meetings took place with the project coordinator (Mathias Engelbeen). Based on preliminary results, and in agreement with the coordinator and the members of the steering committee, some changes were made in the methodology originally proposed and in the definition of the deliverables to be produced. More detailed specifications for each deliverable were also defined via discussions with the coordinator.

1. Estimating the area covered by urban green and mapping of its spatial distribution

The first objective of the project was to use recent high resolution remote sensing data available for the Brussels Capital Region for mapping the spatial distribution of urban green. For this part of the work use was made of an ortho-rectified Quickbird image mosaic acquired between May 20th and June 2nd 2008, with a spatial resolution of 2.4m, produced by GIM. Figure 1 shows an extract of the mosaic with UrbIS road segments superimposed, demonstrating the quality of the geometric correction procedure. The figure however also shows that in some parts of the region the image mosaic does not perfectly coincide with the administrative boundaries of the capital. This implies that estimates of the total areal coverage of urban green for the region may be slightly biased by these discrepancies.

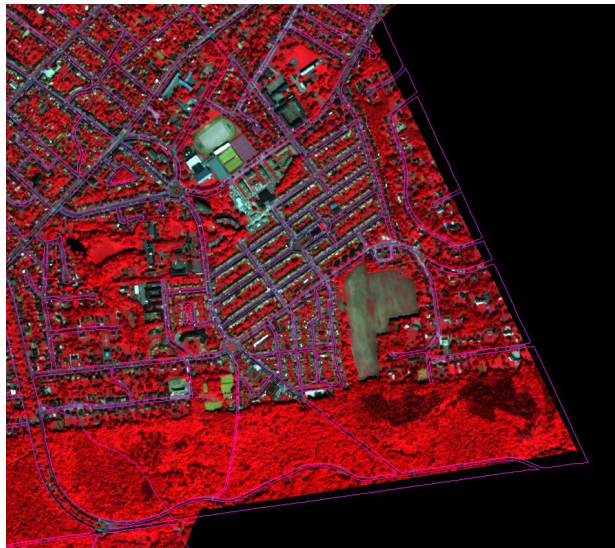


Figure 1. Extract of the Quickbird image mosaic with UrbIS street network superimposed

Mapping of urban green based on the Quickbird image mosaic was accomplished in two steps: first an urban green mask was produced distinguishing between green and non-green areas, by vegetation

index thresholding. A comparison of two frequently used indices, NDVI and MSAVI (Qi et al., 1994), indicated that NDVI performs much better in picking up vegetation in shadow areas than MSAVI. Considering the omnipresence of shadow patches within the urban area the vegetation mask was produced based on NDVI, using an NDVI threshold value of 0.275. In a second step a distinction was made between open and dense vegetation. This was accomplished by assigning all the image pixels within the vegetation mask to one of both classes, based on spectral information and image texture (local variance).

Visual comparison with large-scale aerial photographs indicates that green areas can be delineated with high accuracy on high resolution Quickbird imagery, using the value of the NDVI to distinguish green from non-green areas. Mapping of the green areas for the whole region based on NDVI thresholding shows that 54% of the area of the region is covered by vegetation (table 1). Mapping of dense versus open vegetation indicates that the major part of the green area consists of dense vegetation types (mostly trees), which cover 44.25% of the area. Open vegetation makes up only 9.75% of the area of the capital. For calculating the area figures in table 1, agricultural parcels identified in the green network layer available for Brussels were superimposed on the vegetation layer derived from the satellite image. If parcels were not identified as green through analysis of the satellite image they were added to the open green class, assuming that these parcels were only temporarily left bare, this to reduce the impact of seasonal changes in the estimation of green areas due to crop rotation cycles. It should be mentioned however that not all agricultural fields in the Brussels region are included in the green network. As such seasonal changes in green coverage due to agricultural activities could not be fully taken into account.

	Area (ha)	% of total area
Green spaces	8713.94	54%
Open vegetation	1572.18	9.75%
Dense vegetation	7141.76	44.25%

Table 1. Total area of green space, open and dense vegetation in the Brussels Capital Region, derived from Quickbird imagery

By crossing the vegetation layer derived from the satellite imagery, and corrected for seasonal changes due to agricultural activity, with the urban blocks (Bl) and street surfaces (SS) layer from UrbIS, the percentage of green area for each urban block, as well as for each street surface object can be calculated. The density of vegetation within the UrbIS blocks (figure 3) indicates that while the Brussels region has a relatively high vegetation cover on average, green is mostly concentrated in the periphery, and especially in the eastern and south-eastern part of the city. Mapping the density of urban green at the level of street surface objects (figure 4) clearly shows the presence of green along major axes connecting the centre with the periphery of the city (Avenue Louise, Avenue Roosevelt, Avenue de Tervueren, Avenue Leopold III, Chaussée d’Anvers – Avenue du Port, Avenue Van Volxem – Avenue du Globe), as well as along axes aligned with the pattern of concentric development of the city, such as the Lambermont-Wahis axis in the Northeast, the Boulevard du Woluwe – Boulevard du Souverain axis in the East and Southeast, the Avenue Churchill – Avenue Albert axis in the South, connecting the Bois de la Cambre with the park of Forest and the Park Duden, and the Mettewie – Groeninckx-De May axis in the East, connecting the Elisabeth Park in Koekelberg with the Astrid Park in Anderlecht. Figure 4 also clearly shows the multitude of small green squares present in the densely built 19th century quarters surrounding the city centre.

2. Analyzing the pattern of urban green using spatial metrics

One of the major impacts of urbanization is the fragmentation of open spaces into smaller and more isolated patches. Increased fragmentation of green in urbanized areas can reduce intra- and inter-species connectivity and lead to a loss of biodiversity (Kettunen *et al.*, 2007). Fragmentation of green areas and distance between habitat patches is thus an important factor in determining biodiversity. A *Green*

Infrastructure approach, linking parks and other green spaces, is therefore considered essential for the preservation of biodiversity and to counter further habitat fragmentation (Sylwester, 2009). Fragmentation and isolation of urban green spaces can be described by means of spatial metrics, i.e. quantitative measures of spatial pattern that were originally developed by landscape ecologists to examine the link between the spatial patterning of ecosystem types in natural landscapes and ecological processes (Turner, 1989, 1990). Many metrics have been developed for characterizing patterns in landscapes and were later implemented in the spatial analysis program FRAGSTATS by McGarigal and Marks (1995), which today is a commonly used quantitative tool in the field of landscape ecology.

In this study various spatial metrics available in FRAGSTATS were calculated to describe fragmentation and isolation of open and dense vegetation patches in the Brussels Capital Region, mapped from high resolution Quickbird data. Fragmentation can be described by the total number of patches and by summary statistics characterizing the frequency distribution of patch size (expressed in hectares), including mean patch size, median patch size, standard deviation of patch size and coefficient of variation. Isolation of open and dense patches can be described by two indicators: the Euclidean nearest neighbour distance of a patch to other patches of the same type, and the proximity index.

The Euclidean nearest neighbour distance of a patch i (ENN) is defined by:

$$ENN_i = h_i$$

with h_i the distance from patch i to the nearest neighbouring patch of the same type, based on patch edge-to-edge distance, computed from cell centre to cell centre (figure 2).

ENN is an easily interpretable measure of the isolation of a patch. Its main disadvantage is that it does not fully account for the context of a patch, as it is based on distance to the nearest patch only.

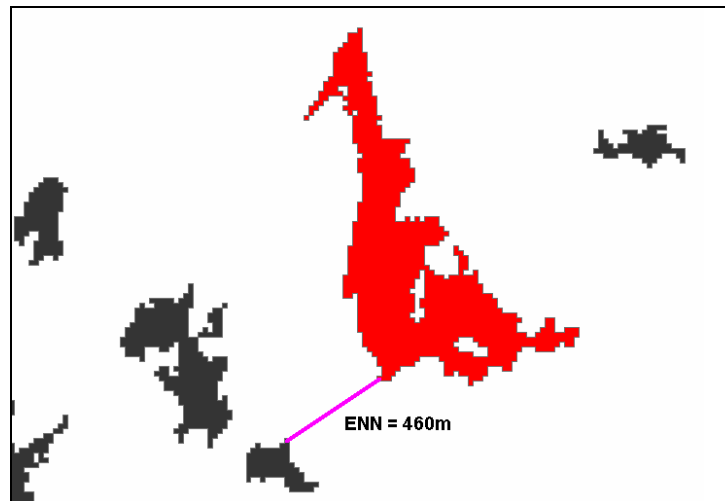


Figure 2 . Euclidean nearest neighbour distance (*ENN*) of the red highlighted patch

Proximity (*PROX*) for a patch i is defined by (figure 5):

$$PROX_i = \sum_{s=1}^n \frac{a_{is}}{h_{is}^2}$$

where:

a_{is} = area (m^2) of patch is within a specified neighbourhood around patch i ,

h_{is} = distance (m) between patch i and patch is , based on patch edge-to-edge distance, computed from cell centre to cell centre,

n = the number of patches within the specified neighbourhood.

The neighbourhood of a patch is defined by a circular region with a user-specified radius.

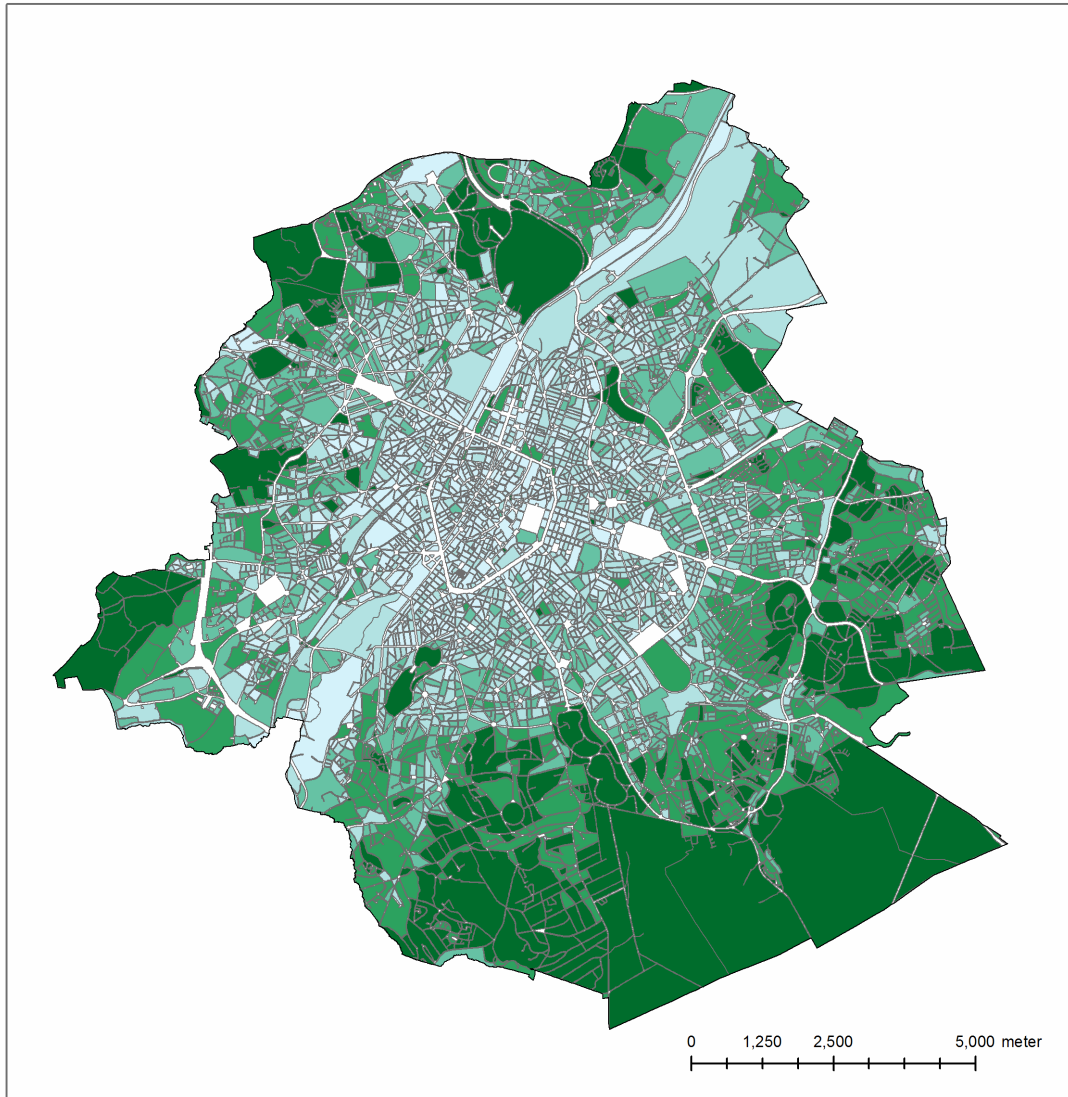


Figure 3. Fractional coverage of green within UrbIS blocks (BI)

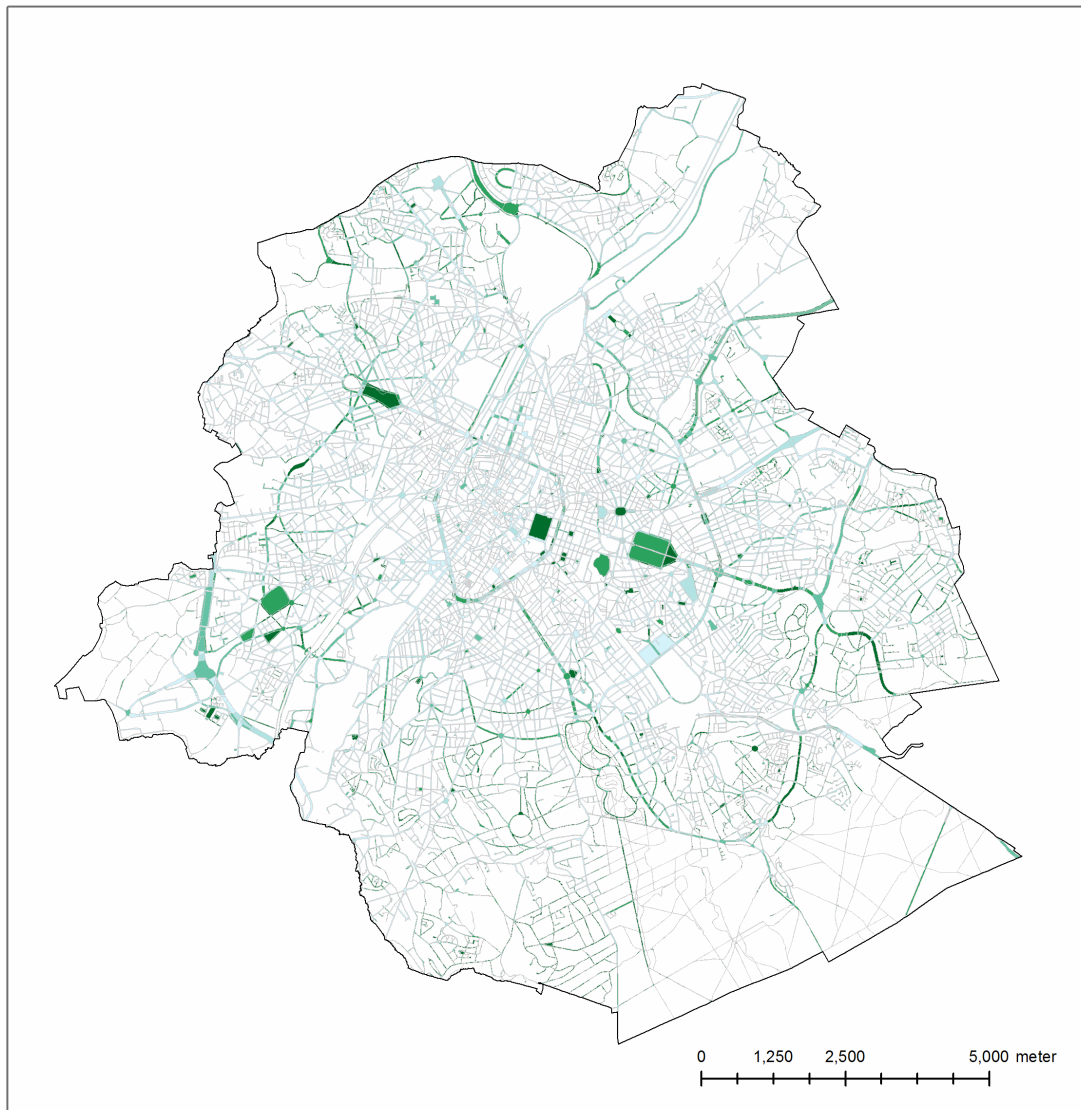


Figure 4. Fractional coverage of green within UrbIS street surface objects (SS)

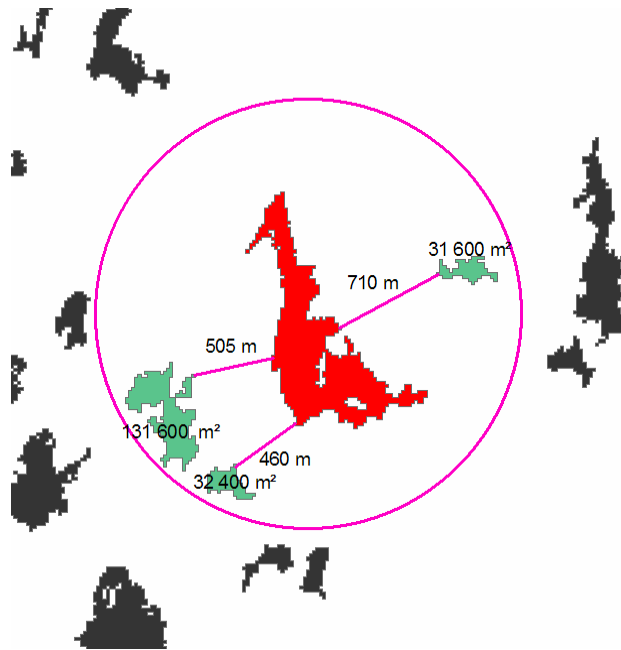


Figure 5. Proximity index for the red patch with a specified radius (purple) is 0.7318

PROX was developed by Gustafson and Parker (1992) to improve upon the simplification that takes only the nearest patch into account for quantifying isolation. The index represents the ecological neighbourhood of a patch more fully by incorporating the distance to all patches within a specified radius and by also taking the area of the surrounding patches into account. The area of neighbouring patches is important because a nearby small patch is considered less significant for determining effective isolation than a large patch that is located slightly further away. *PROX* quantifies the spatial context of a patch in relation to its neighbours. Sparse distributions of small patches are distinguished from configurations where larger patches form a complex cluster. All other things being equal, a patch located in a search radius containing more patches will have a larger *PROX* value. A patch located within a neighbourhood consisting of larger, more contiguous or closer patches will also have a larger index value. *PROX* therefore measures both the degree of patch isolation and the degree of fragmentation within the specified neighbourhood around a patch.

In contrast with *ENN*, the *PROX* metric is less straightforward to interpret. Because it depends on the area of neighbouring patches, as well as on their distance to the focal patch, its absolute value has no direct meaning. However, comparing values for the *PROX* index for individual patches, or summary statistics calculated over all patches of the same type (mean value, median, standard deviation, coefficient of variation) gives a good indication of the relative degree of isolation of an individual patch or a group of patches of the same type (open, dense), or of how the degree of isolation varies between patches of the same type.

Before calculating spatial metrics at patch level, the original vegetation map obtained from the satellite imagery (raster map with a spatial resolution of 2.4m) was generalised using a minimum mapping unit of 100 pixels within urban blocks, and a minimum mapping unit of 50 pixels on roads, respectively corresponding to minimum patch sizes of 576m² and 288m², both for open and dense vegetation. From the patches obtained, only the patches larger than 0.5ha were used for calculating metric values for open vegetation. For dense vegetation, metrics were calculated for minimum patch sizes of 0.5ha, 3ha and 5ha. Metrics were calculated for the Brussels Capital Region as a whole, as well as for 4 peripheral zones, located NW, NE, SW and SE of the city centre, which have been defined by BIM as biological sub-regions. The NW, NE and SW regions have a rural influence, the SE region has a forest influence.

Table 2 shows the total number of patches and the summary statistics for patch size, which give an indication of the fragmentation of vegetation patches, for the Brussels Capital Region as a whole, and for

the 4 sub-regions. When looking at the results for open vegetation for the region as a whole it is immediately clear that open vegetation areas are highly fragmented. The region counts 350 open vegetation patches larger than 0.5ha, with an average size of 1.80ha. Half of these patches are smaller than 0.84ha, pointing at a highly skewed size distribution characterized by a majority of small patches and relatively few larger patches. For three of the four sub-regions (NE, SW, SE) the mean patch size is close to 1ha. While also the NW region is dominated by small open patches, the mean patch size is significantly higher than in the other regions (3.31ha) due to the presence of larger agricultural plots. This also leads to a much higher variation in patch size within this region, as demonstrated by the standard deviation of patch size (5.71ha) which is 4 to 7 times higher than in the other regions.

Patch size statistics for dense vegetation strongly depend, of course, on the minimum patch size applied for calculating the metrics. Using a minimum patch size of 0.5ha, a total of 1687 dense vegetation patches is obtained for the region as a whole. While also for dense vegetation highly skewed patch size distributions are obtained that are dominated by a large number of small patches, both at the level of the region, as well as for the sub-regions, fragmentation is less than for open vegetation. Mean patch size for the entire region is 3.54ha, and reaches its maximum value in the SE region (5.96ha), which incorporates part of the Sonian Forest. While the variation in patch size is limited for the other three regions (SD less than 6ha), in the SE region it is substantial (SD=36ha) due to the presence of large patches of trees in the Sonian Forest. The extreme variation of patch size in this region is also demonstrated by a coefficient of variation (CV) of more than 600%.

	NP	AREA MN (ha)	AREA SD	AREA MD	AREA CV
Brussels open 0.5ha	350	1.8037	3.3641	0.8366	186.5069
NW open 0.5ha	85	3.3074	5.7069	1.084	172.5478
NE open 0.5ha	73	1.1373	0.9214	0.8306	81.0176
SW open 0.5ha	31	1.0843	0.8363	0.826	77.1274
SE open 0.5ha	71	1.096	1.509	0.6854	137.6855
Brussels dense 0.5ha	1687	3.5414	21.3216	1.1555	602.0748
NW dense 0.5 ha	153	2.7717	5.7719	1.156	208.2411
NE dense 0.5 ha	268	2.4913	3.7674	1.1748	151.225
SW dense 0.5 ha	134	3.4659	5.3234	1.6834	153.5944
SE dense 0.5 ha	548	5.9626	36.4135	1.5342	610.6984
Brussels dense 3 ha	352	12.6246	45.5305	5.6123	360.649
NW dense 3ha	31	9.1456	10.5712	4.9219	115.5879
NE dense 3 ha	57	7.478	5.8118	5.1967	77.718
SW dense 3ha	43	8.0548	7.5096	4.8707	93.2322
SE dense 3ha	160	17.4291	65.9896	6.0771	378.617
Brussels dense 5 ha	205	18.9025	58.8637	8.4712	311.4074
NW dense 5ha	14	15.3397	13.3014	8.7278	86.7128
NE dense 5ha	31	10.5849	6.383	8.1867	60.3026
SW dense 5ha	22	11.9809	8.8516	8.3301	73.881
SE dense 5ha	104	24.7312	80.913	7.9286	327.1692

Table 2. Number of patches (NP) and summary statistics for patch size: mean patch size (AREA MN), standard deviation (AREA SD), median (AREA MD) and coefficient of variation (AREA CV)

Putting the threshold for patch size at 3ha or 5ha, which may seem more logical for dense vegetation, given the minimum patch size needed for properly providing ecosystem functions and services, leads to similar results as for a 0.5ha threshold. Patch size distributions remain skewed, with mean patch sizes higher than the median value. The total number of patches is, of course, substantially reduced compared to the 0.5ha scenario. For a 3ha threshold only 352 dense vegetation patches remain for the whole region, for a 5ha threshold only 205 patches remain. Average patch size increases to 12.62ha for the 3ha scenario and to 18.90ha for the 5ha scenario. Again mean patch sizes are similar for

the NW, NE and SW regions, and substantially higher for the SE region. Because the large number of small patches present in the 0.5ha scenario are removed, the variation in patch size, expressed by the standard deviation, increases for the 3ha and 5ha scenario compared to the 0.5ha case. The coefficient of variation, however, which gives a better account of patch size variation, as it is independent of the average size of the patches, reduces to values below 100% for the 5ha scenario, except for the SE region, where it reaches a value of 327%, almost half of the value obtained for the 0.5ha scenario (611%).

The strong fragmentation in terms of number of patches and mean patch size within urban areas is, of course, to a large extent determined by the structure of the road network and the morphology of the built-up area, which partitions the urban space into a large number of green and non-green areas. Calculating metrics related to patch size distribution may therefore give a biased impression of the connectivity of green areas within an urban context. Indeed, green patches that are separated from one another by a dividing road will in many cases be considered as connected, the road not posing a real obstacle to the green area as a whole in fulfilling its ecological functions and services. To take this into account, table 3 shows the fraction of patches of open and dense vegetation that are less than 10m separated from a neighbouring patch of the same type. As can be seen, for open vegetation only a limited fraction of the patches is found within a distance of 10m from other open patches, except in the NW region, where 49% of the open vegetation patches is less than 10m away from another open patch. The majority of these patches are part of the agricultural area in the western part of the commune of Anderlecht.

	NP	NP <10m	NP >=10m	% <10m	% >=10m	ENN MN	ENN STD	ENN MD	ENN CV
Brussels open 0.5ha	350	68	282	19.43%	80.57%	171.16	211.80	86.03	123.75
NW open 0.5ha	85	42	43	49.41%	50.59%	109.18	149.69	44.12	137.11
NE open 0.5ha	73	8	65	10.96%	89.04%	134.54	134.30	96.48	99.82
SW open 0.5ha	31	2	29	6.45%	93.55%	120.60	129.07	79.24	107.03
SE open 0.5ha	71	2	69	2.82%	97.18%	286.27	251.79	232.84	87.96
Brussels dense 0.5ha	1687	1150	537	68.17%	31.83%	47.10	56.43	29.00	119.82
NW dense 0.5 ha	153	97	56	63.40%	36.60%	41.82	36.41	24.17	87.08
NE dense 0.5 ha	268	216	52	80.60%	19.40%	31.79	34.68	20.08	109.09
SW dense 0.5 ha	134	114	20	85.07%	14.93%	27.69	16.83	22.56	60.76
SE dense 0.5 ha	548	457	91	83.39%	16.61%	30.83	14.90	28.80	48.33
Brussels dense 3 ha	352	280	72	79.55%	20.45%	147.37	178.71	68.95	121.26
NW dense 3ha	31	18	13	58.06%	41.94%	254.26	188.24	134.49	74.03
NE dense 3 ha	57	42	15	73.68%	26.32%	170.82	145.46	181.29	85.15
SW dense 3ha	43	40	3	93.02%	6.98%	69.40	51.69	41.91	74.48
SE dense 3ha	160	140	20	87.50%	12.50%	62.91	52.91	42.65	84.10
Brussels dense 5 ha	205	148	57	72.20%	27.80%	167.07	236.39	60.00	141.49
NW dense 5ha	14	4	10	28.57%	71.43%	316.29	350.93	134.49	110.95
NE dense 5ha	31	16	15	51.61%	48.39%	102.80	96.02	62.26	93.40
SW dense 5ha	22	18	4	81.82%	18.18%	57.44	45.96	50.22	80.02
SE dense 5ha	104	92	12	88.46%	11.54%	130.72	183.35	39.14	140.26

Table 3. Total number of patches (NP), number of patches less than 10m and more than 10m separated from a neighbouring patch (NP<10m, NP>=10m), and summary statistics for Euclidean nearest neighbour distance (ENN) for all other patches: mean ENN (ENN MN), standard deviation (ENN SD), median (ENN MD) and coefficient of variation (ENN CV)

For dense vegetation patches, which cover a substantially bigger part of the Brussels Capital Region than open vegetation, a large fraction of the patches is located within 10m from another dense vegetation patch. For the 0.5ha analysis, in the NE, SW and SE sub-regions more than 80% of the patches have a neighbouring patch within 10m distance. In the NW region direct connectivity of patches is less, although still more than 60% of the patches are closely connected. For the 3ha scenario connectivity of patches within a distance of 10m for the SW and SE region is even higher than in the 0.5ha case (93% and 88% within a 10m distance from a neighbouring patch respectively). At the level of 5ha patches this high level of connectivity is maintained in the SE region, while in the SW region it decreases from 93% to 82%. In the NW and NE regions direct connectivity rapidly drops as the minimum size of patches taken into account is increased from 0.5ha to 3ha to 5ha, with in the NW region only 29% of the patches larger than 5ha directly connected to a neighbouring patch. This clearly demonstrates the scale dependency of the spatial pattern.

To explore patch isolation over larger distances, summary statistics of Euclidean nearest neighbour distance (*ENN*) were calculated for the different scenarios based on all the patches that do not have a neighbour within a 10m distance. *ENN* distance also tends to produce a highly skewed distribution, indicating a tendency for clustering of patches (figure 6). At the 0.5ha level spatial clustering of open vegetation patches is clearly less pronounced than for dense patches, with a mean distance between a patch and its nearest neighbour of 109m in the NW region up to 286m in the SE region for open patches against mean nearest neighbour distances between 28m and 42m for dense patches (table 3). Increasing the scale level for dense vegetation to patches with a minimum size of 3ha and 5ha, thus limiting the number of patches that are not directly connected to 20 or less in each of the sub-regions, increases mean *ENN* values, yet on the average patches are still well connected with a maximum value for the mean nearest neighbour distance of 254m (3ha scenario) and 316m (5ha scenario) for the NW region.

Figure 7 shows the spatial distribution of open vegetation patches larger than 0.5ha. As can be seen spatial clustering of open patches is much less pronounced than one might expect from the *ENN* frequency distribution, except in the agricultural area in the NW region. Figure 8 shows the spatial distribution of dense vegetation patches larger than 5ha. Dense patches clearly seem less isolated than open vegetation patches. As can be seen only a small fraction of the patches does not have any other dense vegetation patch within close distance. This is confirmed by the *ENN* summary statistics.

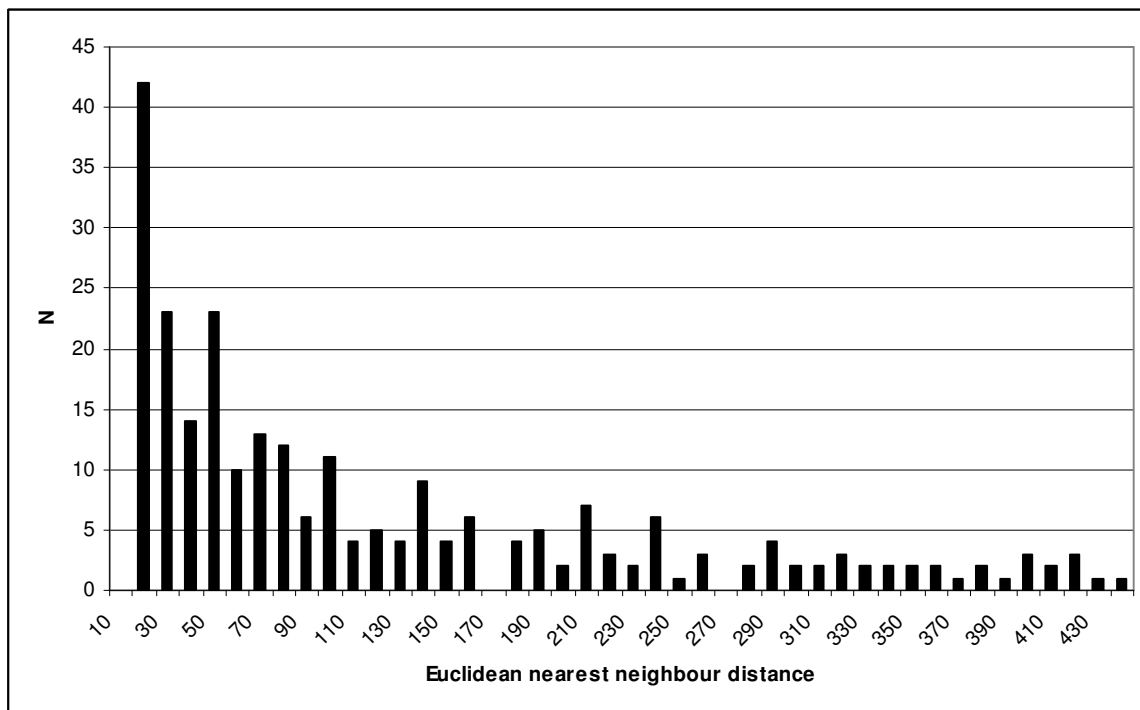


Figure 6. Frequency distribution of Euclidean nearest neighbour distance for open vegetation patches more than 10m separated from their closest neighbour

However, the *ENN* statistics do not fully explain the differences in the degree of clustering between the regions that are clear from the map. While the mean *ENN* value for the NE region (103m) is less than the mean *ENN* value for the SE region (131m), the dense green area in the SE region seems more compact, resulting in a better connectivity between the patches. This is not reflected in the *ENN* summary statistics. This can be explained by the fact that *ENN* statistics are based on the distance to the nearest patch and do not consider the position of the patch in relation to the distribution of patches of the same type in the surrounding area.

Because Euclidean nearest neighbour distance does not provide a good description of the context of a patch, we also calculated the proximity index (*PROX*) for each open and dense vegetation patch included in the analysis. Calculation of the *PROX* index requires the specification of a radius defining the circular neighbourhood around the focal patch for which the index is determined. While the choice of the radius is somewhat arbitrary, it may have a substantial impact on the value of the *PROX* index. In the absence of clear guidelines for defining the neighbourhood of a patch the radius was set to 500m. This choice was based on the frequency distribution of *ENN* distances, ensuring that for each scenario almost all of the patches (except a few outliers) have a least one other patch present within their circular neighbourhood.

Table 4 shows the summary statistics of *PROX* for each scenario. As can be seen, for open vegetation patches results for the NW region differ substantially from the results obtained for the other three regions, with a mean value for the *PROX* index for the NW region larger than 4000 against mean values for the other regions around 50 or less. Also in this case the frequency distribution proves to be strongly skewed with a median value of 232 for the NW region and values of less than 3 for the other regions. This demonstrates that even if based on nearest neighbour distance open patches seem well connected, this is not the case, except for the NW region. This observation is confirmed by the spatial distribution of open patches shown in figure 7. Mean values of the *PROX* index for dense vegetation patches for the 0.5ha scenario show that dense vegetation is much more clustered than open vegetation, except in the NW region where mean *PROX* values for open and dense vegetation are similar. The high mean value of the *PROX* index for the SE region (close to 40000 and 4 to nearly 10 times higher than for the other regions) is indicative of the strong presence and spatial clustering of dense vegetation in and around the Sonian Forest.

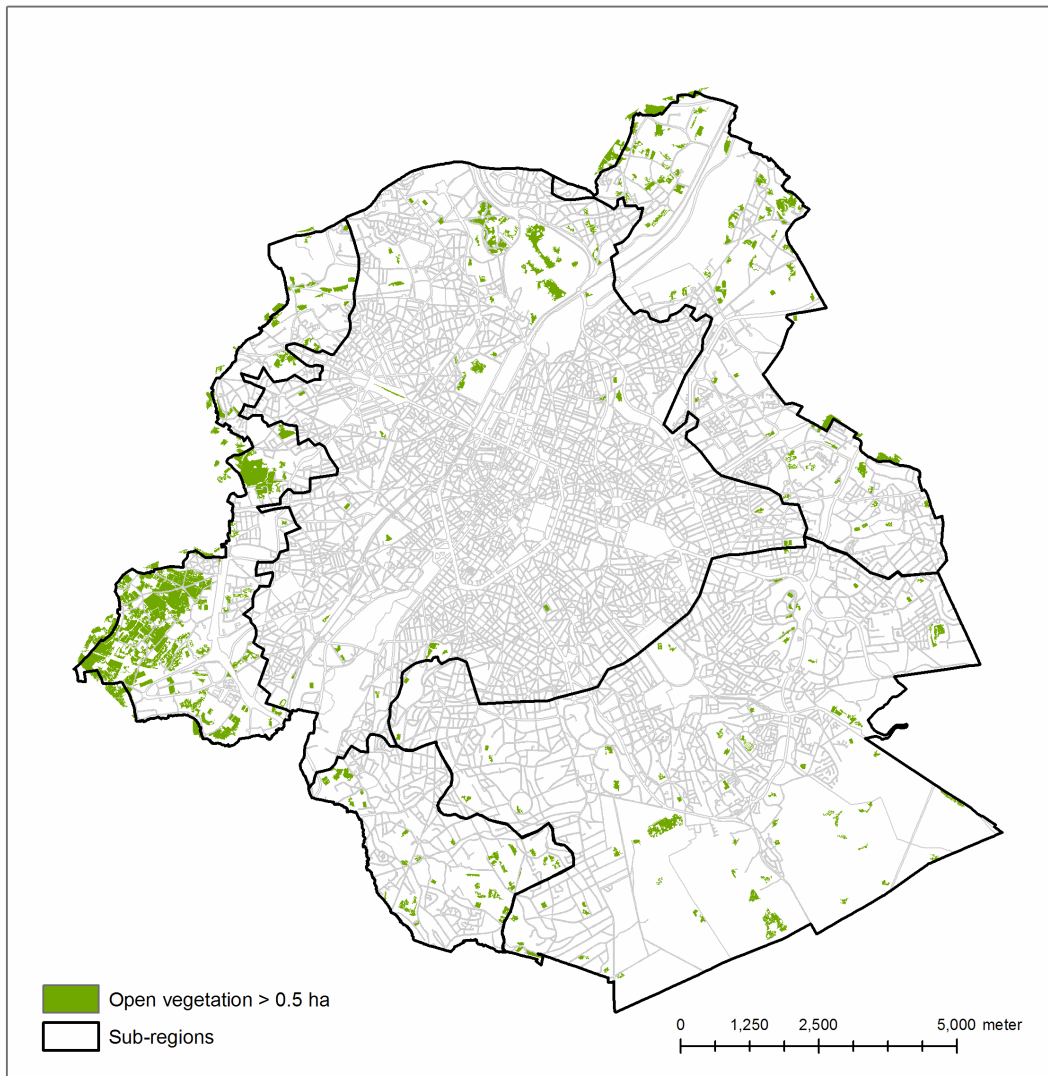


Figure 7. *Spatial distribution of open vegetation patches with a minimum size of 0.5 ha*

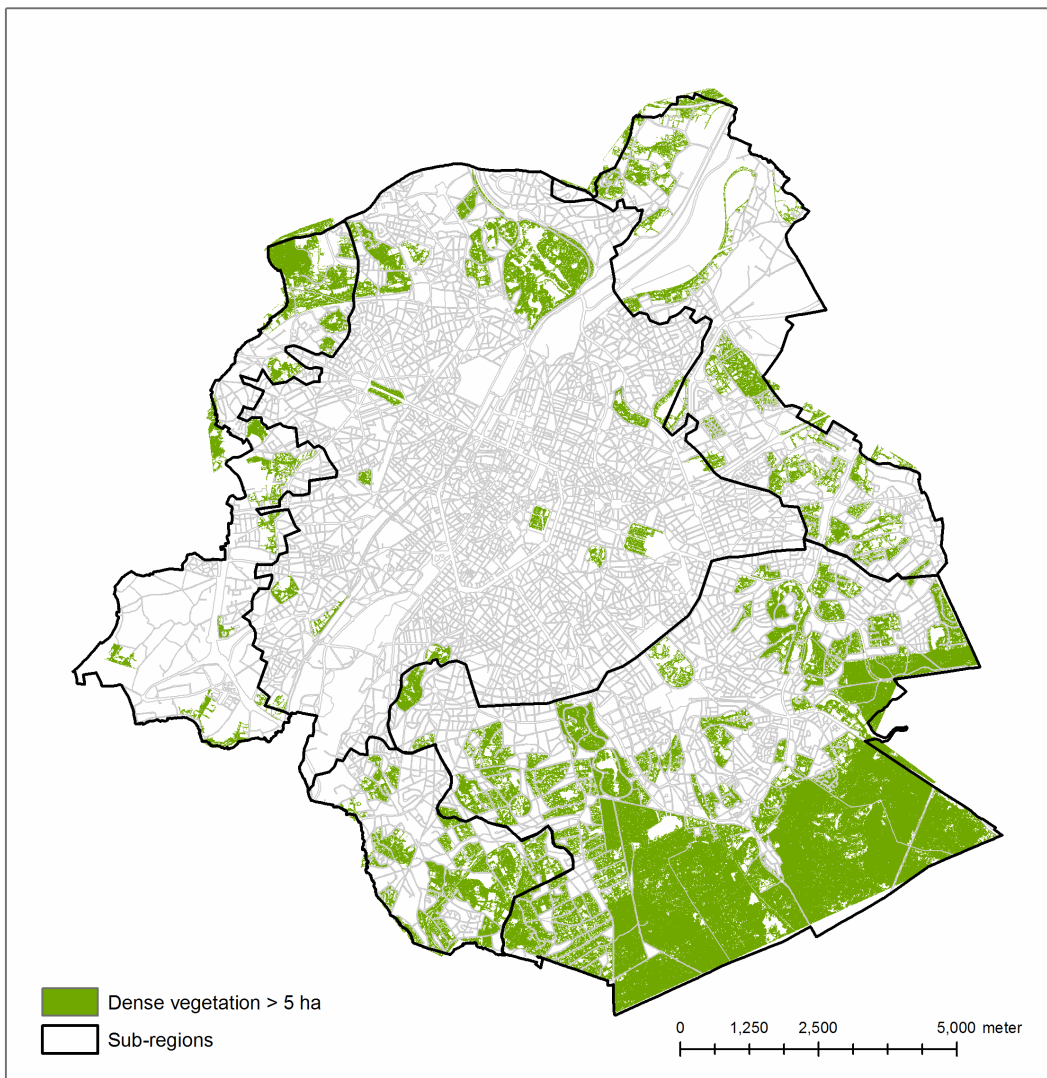


Figure 8. Spatial distribution of dense vegetation patches with a minimum size of 5ha

	NP	PROX MN	PROX SD	PROX MD	PROX CV
Brussels open 0.5ha	350	1158.64	4908.56	5.17	423.65
NW open 0.5ha	85	4157.66	8585.55	232.03	206.50
NE open 0.5ha	73	55.45	186.03	2.73	335.46
SW open 0.5ha	31	31.36	87.16	2.48	277.90
SE open 0.5ha	71	32.74	162.59	0.28	496.55
Brussels dense 0.5ha	1687	16273.97	70176.45	1557.99	431.22
NW dense 0.5 ha	153	4454.36	9299.68	658.25	208.78
NE dense 0.5 ha	268	4674.15	6734.54	2027.27	144.08
SW dense 0.5 ha	134	10940.15	14618.61	7029.04	133.62
SE dense 0.5 ha	548	38985.44	118393.28	6189.87	303.69
Brussels dense 3 ha	352	45012.76	123131.79	9996.17	273.55
NW dense 3ha	31	10887.26	15863.44	2941.87	145.71
NE dense 3 ha	57	7722.11	9669.11	4487.58	125.21
SW dense 3ha	43	18696.36	20742.52	7515.28	110.94
SE dense 3ha	160	82844.35	173382.98	20739.22	209.29
Brussels dense 5 ha	205	61510.24	147902.72	14415.09	240.45
NW dense 5ha	14	12081.83	19272.82	13.43	159.52
NE dense 5ha	31	8014.74	11491.37	914.28	143.38
SW dense 5ha	22	24352.94	23291.43	17531.24	95.64
SE dense 5ha	104	105634.23	195756.68	24862.53	185.32

Table 4. Total number of patches (NP) and summary statistics for the proximity index (PROX): mean PROX (PROX MN), standard deviation (PROX SD), median (PROX MD) and coefficient of variation (PROX CV)

Increasing the minimum patch size for dense vegetation to 3ha and 5ha substantially increases the mean values for the *PROX* index, showing that large patches are more strongly connected than smaller patches. This strong clustering is apparent from the spatial distribution of dense vegetation patches shown in figure 8.

3. Occurrence of open/dense vegetation, non-vegetated areas and water within the mapping units of the “Biologische waarderingskaart”

Based on the mapping of open and dense vegetation from the Quickbird image, and the presence of water surfaces as documented in UrbIS, the % of open/dense vegetation, non-vegetated areas and water was determined for each polygon in the “Biologische Waarderingskaart” (BWK) and added as attributes to the BWK vector layer. Aggregating the units of the BWK into 10 major classes and assigning mixed units to the dominant class, produces area fractions for the four major land-cover types as shown in table 5. Care should be taken when interpreting these statistics. First of all, as just mentioned, the predominant vegetation type within a BWK polygon was used to determine the class to which it belongs. In many cases, BWK polygons are an aggregate of several vegetation elements. This is illustrated for an example polygon in figure 9, where the predominant type according to BWK is ‘ha’ (a type of grassland) but 86% of the area is actually covered by dense vegetation due to the presence of trees.

Another thing that should be kept in mind when interpreting the figures in table 5 and the land-cover fractions for individual polygons is the presence of classification errors between open and dense vegetation. While the distinction between green/non-green areas, based on NDVI thresholding (see section 1) can be made in a highly accurate way, distinguishing between open and dense vegetation based on Quickbird’s four spectral bands and the additional use of texture information is more difficult and unavoidably introduces some error.

	Open vegetation	Dense vegetation	Water	Non-green area
Cropland (b)	48.6%	28.7%	0.0%	22.7%
Other mapped features (k)	10.0%	56.2%	0.4%	33.4%
Grassland (h)	46.3%	37.9%	0.1%	15.6%
Heath and thicket (c+s)	8.3%	75.3%	0.0%	16.4%
Deciduous trees (f+q+e+v+r+n)	2.5%	96.2%	0.1%	0.8%
Swamps (m)	10.4%	86.9%	1.7%	1.0%
Coniferous trees (p)	0.2%	99.6%	0.0%	0.2%
Poplars (l)	6.7%	89.3%	0.1%	3.9%
Water (a)	0.3%	5.6%	89.6%	4.5%
Urban (u)	2.5%	34.0%	0.0%	63.4%

Table 5. Fraction of open vegetation, dense vegetation, water and non-green area for major BWK classes

In training the image classifier applied in this study and in evaluating its output, specific attention was paid to properly identifying rows of trees occurring along the road network as dense vegetation. Because the 2.4m pixel size of Quickbird imagery can be considered a critical resolution for picking up the spectral characteristics of individual trees (trees with moderate canopy size will very often only partially cover a 2.4m pixel), some degree of spectral confusion between pixels covered by open and dense vegetation cannot be avoided. Training a classifier to properly identify rows of trees as dense vegetation, even in the case of moderate canopy sizes, automatically implies that in park areas or in agricultural areas some “contamination” of dense vegetation may occur within herbaceous plots and vice versa. This can be noticed in figure 9.

While this “contamination” effect will partly disappear by generalizing the classification result based on the application of a minimum mapping unit (figure 10), as is done in this study, local bias in the calculation of the fraction of open/dense vegetation may remain. This bias will have little impact on the analysis of the overall spatial pattern of open and dense patches (see section 2), yet if one wants to obtain accurate estimates of the area of open and dense vegetation within each individual BWK polygon one should be cautious in using the fractions based on the Quickbird image interpretation. An accurate estimation of different vegetation types within individual BWK polygons would require a thematically more detailed vegetation mapping, which could be achieved by making use of hyperspectral image data.



Figure 9. Extract of the open/dense vegetation map with BWK polygon superimposed (dark green = dense vegetation, bright green = open vegetation, grey = non-green areas)



Figure 10. Extract of the open/dense vegetation map after generalization, with BWK polygon superimposed (dark green = dense vegetation, bright green = open vegetation, grey = non-green areas)

PART II ANALYSIS OF THE EVOLUTION OF NON-BUILT (GREEN) SPACES IN AND AROUND THE BRUSSELS CAPITAL REGION OVER THE LAST DECADES

Objectives

In this part of the project, the temporal evolution of urban green in and around the Brussels Capital Region is examined. Medium resolution (MR) satellite images were used for this purpose because, in contrast with the high resolution data used in part I, this type of imagery has been available since the early 1970's and therefore provides a historical perspective on vegetation cover. Two main types of map products were derived for an image time-series that starts in the late seventies. First, so-called "hard" classifications were developed, which means that pixels were discretely labelled to a single class. The resulting land-cover maps both serve for calculating spatial metrics and for obtaining so-called "soft" classifications. In a soft classification, pixels are not discretely assigned to one particular class. Instead, sub-pixel proportions or land-cover fractions are derived for each pixel. For this study, both fractional sealed surface and vegetation maps were produced. These thematic maps are continuous and provide more information about what happens within the area covered by the pixels. They show vegetation and sealed surface densities, which are useful for a more detailed examination of land-cover changes.

The outline of part II is as follows. In a first section, the image time-series and geometric pre-processing are discussed. The "hard" land-cover maps and the methods used for deriving them are described in the second section. The third section is dedicated to soft classification, while the outcome of the analysis with spatial metrics is discussed in section 4.

1. Time-series of medium resolution data

The evolution of green areas was analysed based on a time-series of MR imagery (table 6). Landsat, Aster and SPOT archives were searched for nearly cloud-free imagery within a time-period from the late 70s to the late 00s with intervals of approximately 10 years. A useful recent Landsat image was unavailable for the study area because of the malfunctioning scan line corrector of the Landsat 7 satellite. This defect causes the occurrence of wedge-shaped stripes in the images. Aster images covering the entire study area were also not available. A SPOT image was therefore acquired to complete the time-series. Although this image has a good overall quality, small cloud patches cover parts of the study area. These clouds and their shadows were digitised into a vector layer to exclude them in the calculation of metric and area statistics. Approximately 1.26% of the study area is covered by clouds or their shadows on the 2008 image.

Sensor	Acquisition date	Spatial resolution
Landsat 2 – MSS	8 October 1978	60m (resampled from 78m)
Landsat 5 - ETM	23 May 1989	30m
Landsat 7 – ETM+	3 July 2001	30m
SPOT 2 - HRV	6 May 2008	20m

Table 6. Time-series of medium resolution images used for temporal analysis of green areas

The four images were set in the Belgian Lambert projection by geometrically co-registering them to the available high resolution (HR) Quickbird image (see part I) with a set of visually selected ground control points. A few points were also selected outside the area covered by the Quickbird image with the aid of digital orthofotos. A second order polynomial function was used for the coordinate transformation, in combination with a resampling technique using bilinear interpolation. The RMS error on check points was kept less than half the size of a pixel for each image. During the resampling process, the images were clipped to the minimum bounding box of the study area, which corresponds to a 5km buffer around the

Brussels Capital Region. During resampling, we made sure that the pixel grids of the four images coincided. This means that 1 Landsat MSS pixel covers exactly 4 Landsat ETM(+) pixels and 9 Spot HRV pixels. The digital numbers of the imagery were converted to at-sensor reflectance, and a brightness normalisation was carried out for the purpose of deriving fractional vegetation and sealed surface cover (see section 3).

2. “Hard” land-cover maps

The objective of this part of the project was to develop a land-cover map for each image (table 6) with 4 main classes: open vegetation, dense vegetation, urban area and water. This was achieved by first applying an unsupervised classification (clustering) approach, which divides the pixels of each image in a number of spectrally distinct classes. Some classes were grouped together or further subdivided with additional clustering based on a visual inspection of the resulting maps. The outcome of this step was then subjected to post-classification analysis in order to remove noise and partly correct classification errors. Noise was removed with a filter that assigns single, spatially isolated pixels to the most frequently occurring class in its neighbourhood. Context-based rules that apply thresholds to size and adjacency of patches were used for correcting larger misclassified patches (Van de Voorde *et al.*, 2007). A rule was defined, for instance, to remove small patches of misclassified water pixels within the urban area. Such misclassification is common and usually results from spectral confusion between water, shadows or dark roofs. The rule defined to solve this issue specifies that water patches smaller than a certain number of pixels should be relabelled to the class “urban” if they are adjacent to urban patches for at least 50% of their circumference. Thresholds for the rules were determined by the analyst based on knowledge of the study area, visual interpretation and common sense spatial logic.

Although many classification errors can be removed using this context-based spatial logic, some problems remain. A common problem with classification of broadband spectral images of urban areas is the confusion between bare soil and certain urban materials. In the images used for this project, this problem manifested itself mainly as bare soil classified as urban rather than the reverse. To correct these errors, ancillary data were used. As the study area covers the three administrative regions of Belgium, these data were obtained from three sources. Vector data with agricultural parcels was used for the parts of the study area belonging to the Flemish and Walloon region. Although these data were available for several years in the past, the most recent version (2009) was used for all images in the time-series because it was also the most complete version. The reason for this is that the polygons present in the databases represent parcels for which the farmers received certain subsidies. As the number of subsidised plots increased with time, the more recent data also contain more parcels. For correcting classification errors between built-up area and bare soil, we assume that land in use for agriculture today was not built-up in the past. This is a reasonable assumption, but the reverse may not be true. Land that is urbanised today, for which bare soil was wrongly classified as built-up in earlier images, cannot be corrected in the historic images with this approach. For the Brussels Region, information on agricultural parcels was not available. Instead, the zonal plan (PRAS/GBP) was used to identify agricultural areas. Because a zonal plan indicates the desired spatial organisation, which not necessarily corresponds to actual land use, the data was visually inspected to remove buildings. Data for the three regions were combined into a single file and rasterised to the image grids for creating a mask of agricultural areas. This mask was then superimposed on the image classifications to change all agricultural pixels that were classified as urban or bare soil into open vegetation.

The accuracy of the method was assessed for the 2008 image with a spatially stratified set consisting of 1883 validation pixels, randomly selected in a rectangular mesh with a cell-size of 1 km². The selected pixels were visually labelled with the aid of the Quickbird image and high resolution imagery from Google Earth. A confusion matrix was then determined based on this validation sample (table 7). Overall, 87% of the samples was attributed to the correct class, with a kappa index of agreement (KIA) of 0.81. The user’s accuracies are relatively high for each class, but the producer’s accuracies for water (62%) and dense vegetation (78%) are relatively low. The confusion matrix indicates that this is caused by misallocating some pixels of these classes to the urban area. The reason for this misallocation is related to the spatial resolution of the sensor. The misclassified dense vegetation samples, for instance,

are mostly located within the dense urban centre and are usually smaller than 4 to 5 SPOT pixels. Water bodies are also often just a few pixels wide, and have a low contrast with the built-up area. These misclassified areas are well below the minimum mapping units that are used to define patches for the analysis with spatial metrics.

		Reference data						
		Open vegetation	Dense vegetation	Urban area	Water	Total	User's accuracy	KIA
Classified data	Open vegetation	319	42	5	0	366	87%	0.86
	Dense vegetation	13	358	0	6	377	95%	0.70
	Urban area	24	57	459	34	574	80%	0.98
	Water	0	0	0	66	66	100%	0.60
	Total	356	457	464	106	1383	PCC: 87%	0.81
	Producer's accuracy	90%	78%	99%	62%			

Table 7 . Confusion matrix for the hard classification of 2008

On the 4 hard land-cover maps (figure 12) we can see that the urban area dominates the centre, as well as the northern and eastern part of the scene. The western part mostly consists of open and half open landscapes, which become more fragmented as time progresses due to urban expansion (figure 13). The southern part of the area is taken up for a large part by the Sonian forest. The forest itself remains unchanged due to its protected status, but to its east and west, urbanisation leaves its mark as patches of dense vegetation are split up by low density residential construction (figure 14).

We should point out, however, that for correctly interpreting these maps possible effects caused by differences in image resolution should be taken into account. The detection and successful mapping of objects on digital imagery strongly depends on their size in relation to the sensor's instantaneous field of view. Some smaller vegetation patches, for instance, are detected on the 2008 SPOT image with a resolution of 20m, but not on the Landsat images with ground resolutions of 30 or 78 meters. This is for instance the case for clearings in the Sonian Forest, which are almost not visible on the classifications derived from the Landsat images.

The hard classifications allow the calculation of area statistics for each date (table 8 and figure 11), which provide a general numerical view on the land-cover changes in the study area. Compared to the vegetation cover within the Capital Region itself (table 1), which is clearly dominated by dense vegetation, the study area defined for part II includes much more open green due to the rural nature of the Brussels urban fringe. During the time-period covered by the images, 4503 hectares of land have become urbanised. This increase is limited between 1978 and 1989, but takes up in pace between 1989 and 2001 (+1707 ha) and between 2001 and 2008 (+2647 ha). Urban growth occurs at the expense of dense and open vegetation. Dense vegetation decreases gradually from 1978 to 2008. Open vegetation appears to increase between 1978 and 1989, which seems to indicate that in this period dense vegetation is converted into open vegetation. Given the relatively low resolution of the 1978 image, however, it is likely part of the changes that are observed between 1978 and 1989 are related to the strong difference in resolution between both images. Indeed, it is obvious that the resolution effect which was discussed above will also influence the calculation of area statistics. Water bodies, for instance, are not detected at all in the classification of the 1978 image due to their relatively low contrast with the urban area and their small scale in relation to the pixel size. Hence changes observed between 1978 and 1989 should be interpreted with caution. Between 1989 and 2008 the urban area steadily increases, while open and dense vegetation decrease. As the imagery for this period is similar in terms of spatial resolution and provides substantially more detail than the 1978 image, the changes over this 20-year period confirm the overall trend of urbanization observed in the urban fringe. We should take into account, though, that not all pixels labelled as "urban" in the hard land-cover maps produced can be interpreted as fully built-up (or "sealed"). Due to the discrete allocation of pixels to a single land-cover class, actual vegetation cover will

be underestimated in the urbanised area. This will become clear in the discussion on soft classification in section 3.

Year	Open vegetation	Dense vegetation	Total vegetation	Urban	Water
1978	15750.00 (30.5%)	12226.68 (23.7%)	27976.68 (54.2%)	23646.60 (45.8%)	0 (0.0%)
1989	16720.11 (32.4%)	10842.03 (21.0%)	27562.14 (53.4%)	23795.19 (46.1%)	268.56 (0.5%)
2001	16082.82 (31.2%)	9802.17 (19.0%)	25884.99 (50.2%)	25502.67 (49.4%)	238.23 (0.5%)
2008*	14124.68 (27.7%)	8421.04 (16.5%)	22545.72 (44.2%)	28149.68 (55.2%)	276.04 (0.5%)

Table 8. Area(hectares) covered by each of the 4 classes throughout the time-series.

* 652.96 hectares were covered by clouds and their shadows in the 2008 image

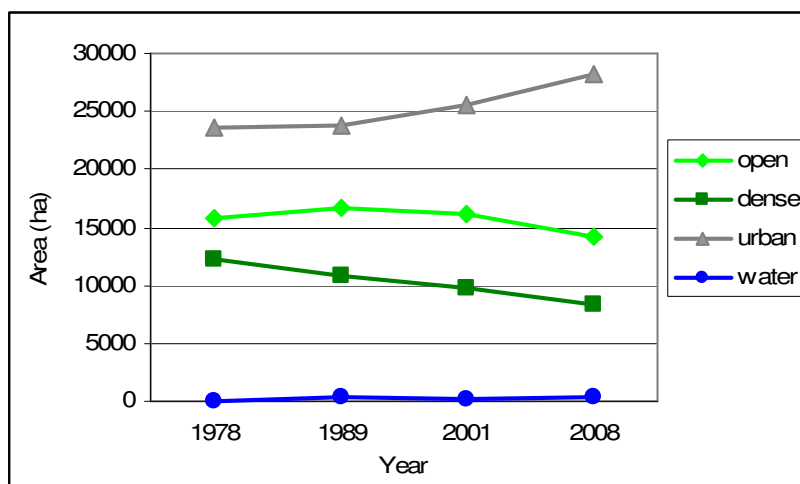


Figure 11. Temporal land-cover trends in the study area

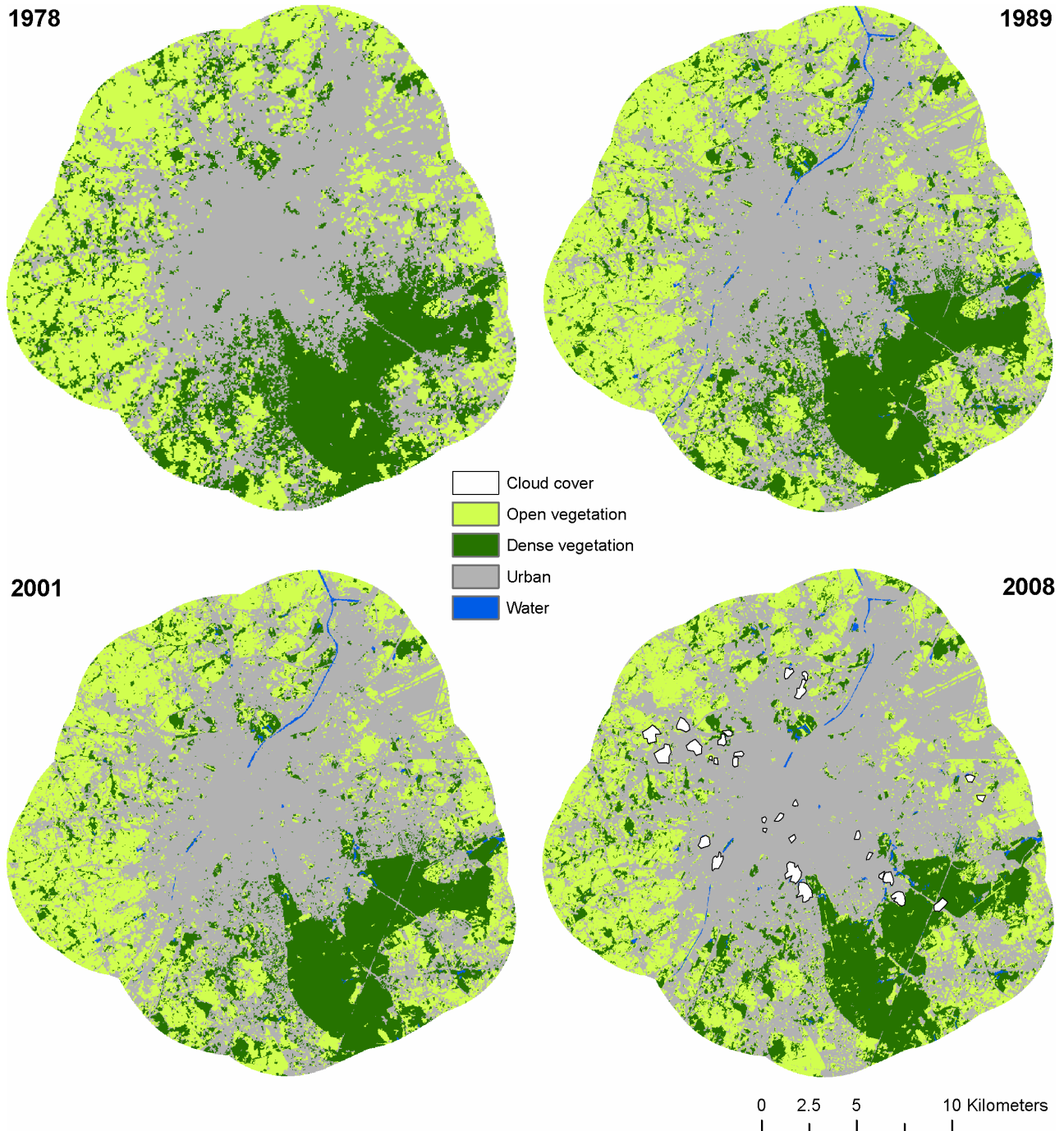


Figure 12. Hard classifications for the images of the time-series

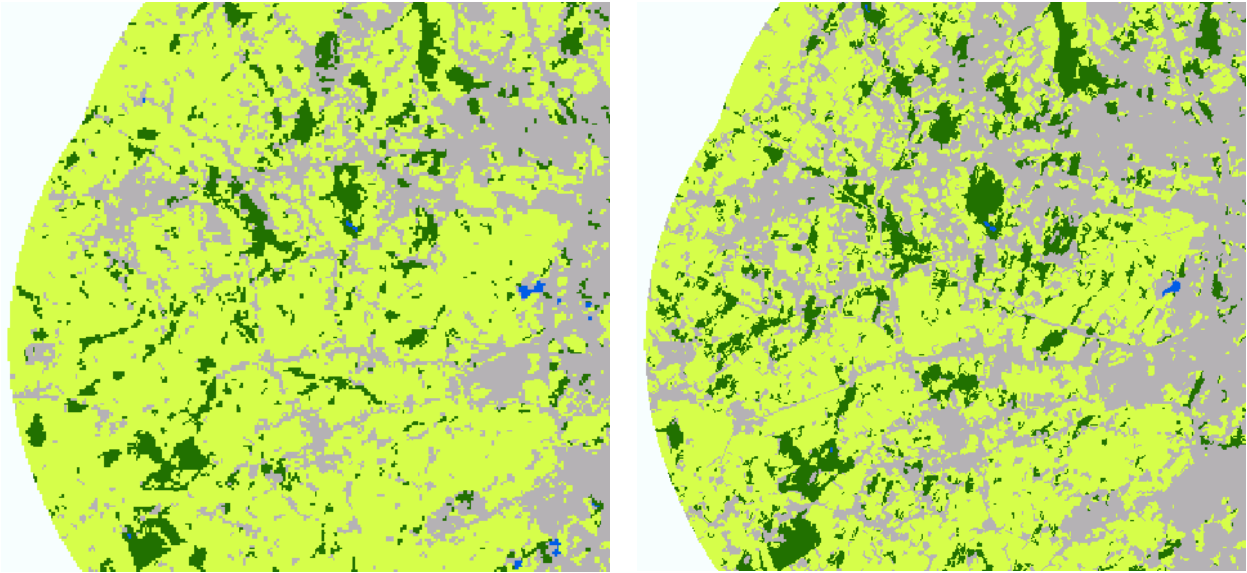


Figure 13. Hard classifications showing the western part of the study area in 1989 (left) and 2008 (right) indicate increasing fragmentation of the open landscape due to urban development

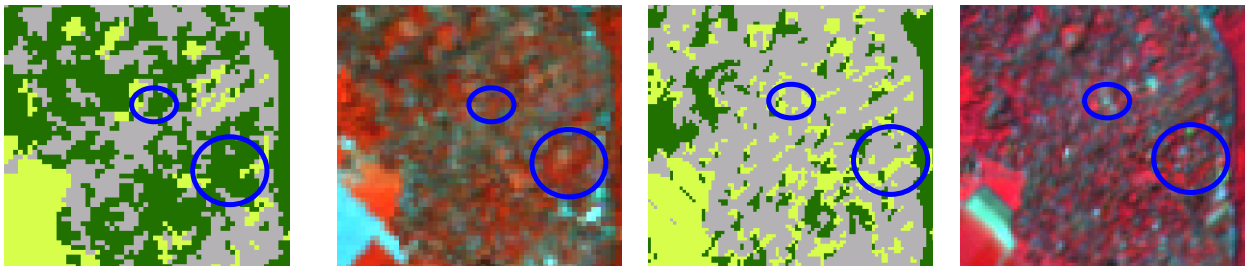


Figure 14. Hard classifications and extracts of the satellite images of 1989 and 2008 showing a part of the scene west of the Sonian forest where urban development dissolves dense vegetation patches.

3. “Soft” vegetation and sealed surface maps derived with sub-pixel classification

Fractional vegetation cover was estimated for each pixel corresponding to the “urban” class in the “hard” land-cover maps discussed in the previous section. Pixels belonging to the classes “open” and “dense” vegetation were considered to be fully covered by vegetation (i.e. 100%), while water pixels were considered as non-vegetated (0%). The estimation of the vegetation proportions within the urban area was achieved with a linear model which was separately developed for each image with stepwise regression analysis (Bauer et al., 2008; Van de Voorde et al., 2008) :

$$V_y = a_{0,y} + a_{1,y}\hat{\rho}_{1,y} + a_{2,y}\hat{\rho}_{2,y} + \dots + a_{n,y}\hat{\rho}_{n,y}$$

with

V_y : the estimated sub-pixel vegetation fraction for year y ,

$a_{i,y}$: the model regression parameters for the image of year y

$\hat{\rho}_{i,y}$: the normalised reflectance of band i for the image of year y and

n : the number of spectral bands used by the stepwise regression analysis.

Developing the model involved relating the image spectral values to known reference proportions for a set of sample pixels that were randomly selected within the urban masks. Reference proportions for regression analysis were obtained from the high resolution Quickbird classification developed in part I. This is possible because each pixel of the MR images covers several HR Quickbird pixels (e.g. 625 in the case of Landsat MSS) and counting the number of high resolution vegetation pixels in a medium resolution pixel provides a vegetation proportion for that pixel. As the Quickbird image was acquired in 2008 and most MR data are much older, a temporal filtering approach was used to select sample pixels that did not change. This approach is based on comparing the normalised difference vegetation index (NDVI) of the MR pixels to the average NDVI of the constituent Quickbird pixels. Pixels for which there is no substantial change in NDVI were considered useful for sampling (Van de Voorde et al., 2009).

The linear models relating sub-pixel vegetation cover to spectral reflectance all use the red and infrared spectral bands, while most other bands were considered superfluous by the stepwise regression analyses. This is not surprising given the fact that the red and infrared bands include most of the information required for discriminating vegetated from non vegetated surfaces. These two bands are also used for calculating NDVI. In addition to the red and infrared bands, the models for 1978 and 1989 use the green band and the model for 2001 also uses ETM band 5 (SWIR). Although these models were developed and applied on the native resolution of the images (20m, 30m, 60m), the resulting fractional vegetation maps (figure 15) were aggregated to 60m resolution, which is the common denominator that allows a pixel-by-pixel comparison of all the maps in the time-series. Sealed surface maps were obtained by subtracting the vegetation fractions from 1 within the bounds of the urban class (figure 16).

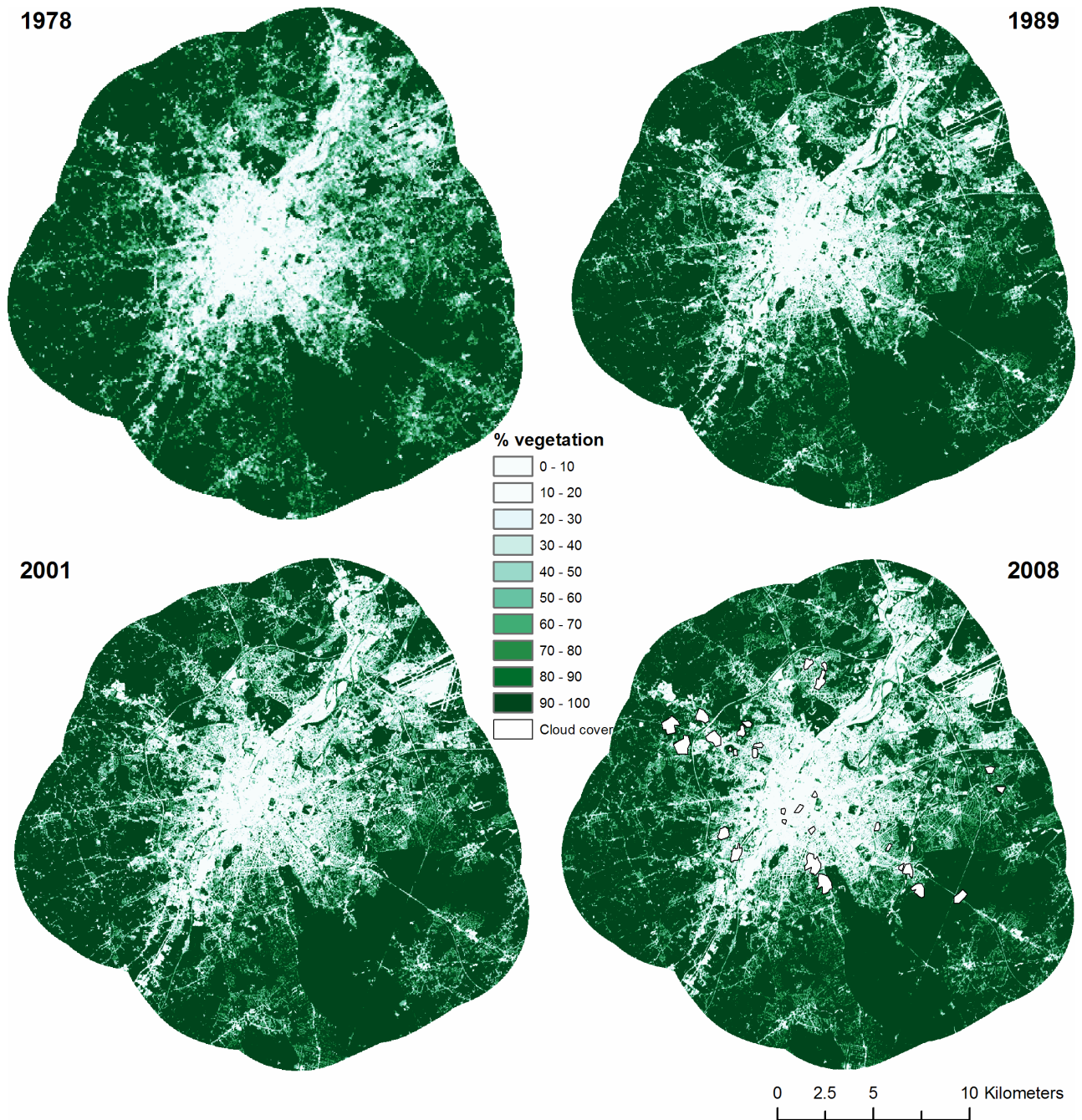


Figure 15. Percentage vegetation cover for each date

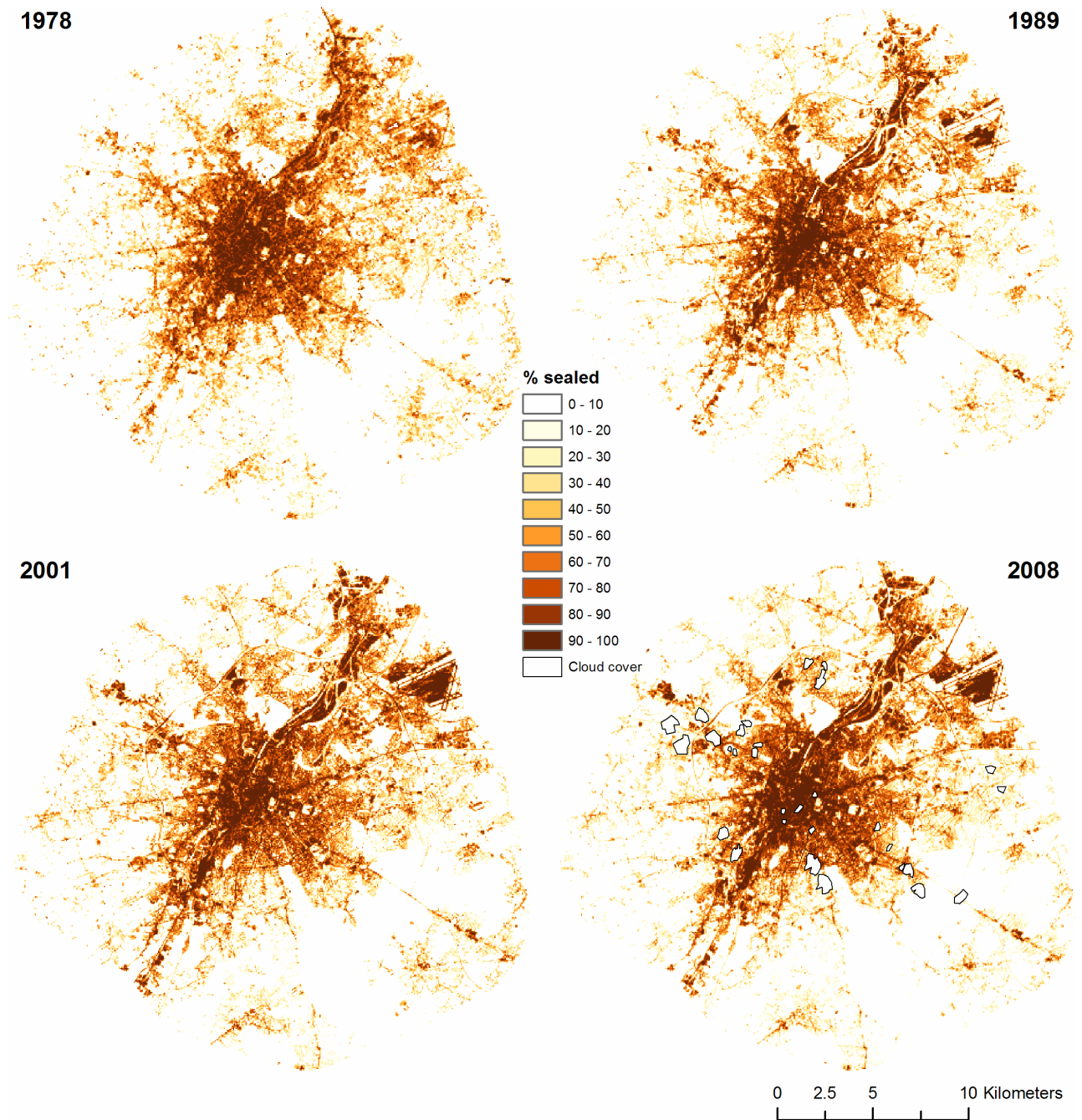


Figure 16. Percentage sealed surface cover for each date

The accuracy of the proportion maps was estimated with an independent validation sample that was obtained in a similar fashion as the sample used to build the models (table 9). Predicted vegetation fractions were compared to reference fractions with three error measures: mean error, mean absolute error and the correlation coefficient. The mean error (*ME*) is used to indicate a possible bias in the proportion estimates (over or underestimation):

$$ME = \frac{\sum_{j=1}^N P'_j - P_j}{N}$$

with

N: the total number of pixels in the validation sample;

P_j: vegetation fraction inside validation pixel *j*, derived from the high resolution Quickbird classification (ground truth);

P'_j: vegetation fraction inside validation pixel *j*, estimated by the sub-pixel regression model.

The mean absolute error of the estimated vegetation fraction (*MAE*) is a measure of the error magnitude:

$$MAE = \frac{\sum_{j=1}^N |P'_j - P_j|}{N}$$

The error magnitude (*MAE*) or average prediction error lies around 13-14% for all models. The correlation between reference proportions and estimated proportions of vegetation proves to be quite high (around 0.80 for all dates in the time series). The relatively small mean errors indicate that the models have little bias and that overestimations in some validation pixels are compensated by underestimation in others.

Year	ME _y	MAE _y	ρ _y	Error variance σ ² _y
1978	0.0125	0.1402	0.8159	0.0301
1989	-0.0192	0.1412	0.7893	0.0329
2001	-0.0056	0.1324	0.8078	0.0300
2008	0.0090	0.13942	0.7903	0.0339

Table 9. Mean error (*ME*), mean absolute error (*MAE*), correlation coefficient (*ρ*) and error variance estimated on an independent validation sample

The proportion maps were used for determining the total area covered by vegetation and sealed surfaces in the study area (table 10, figure 17). In contrast to the area statistics that were calculated for each class on the hard classifications (table 8), the area calculations based on the fractional maps also take sub-pixel land cover of the urban area into account. For this reason, the area covered by vegetation is significantly higher for estimations based on the proportion maps and the decline with time is more moderate (-1903 ha between 1989 and 2008). The relatively moderate decline in vegetation cover in the statistics hides the fact that urban expansion is indeed occurring in the form of low density residential development. This type of land use increases landscape fragmentation and even though vegetation is often abundant in gardens, it is not publicly accessible (or even visible) and usually contains little biodiversity.

Year	Total vegetation	Sealed surfaces	Water
1978	40018.24 (77.5%)	11605.04 (22.5%)	0 (0.0%)
1989	40286.06 (78.0%)	11071.27 (21.4%)	268.56 (0.5%)
2001	38638.18 (74.8%)	12749.48 (24.7%)	238.23 (0.5%)
2008*	38271.95 (75.1)	12445.75 (24.4%)	276.04 (0.5%)

Table 10. Area (hectares) covered by vegetation, sealed surfaces and water throughout the time-series.
* 652.96 hectares were covered by clouds and their shadows in the 2008 image

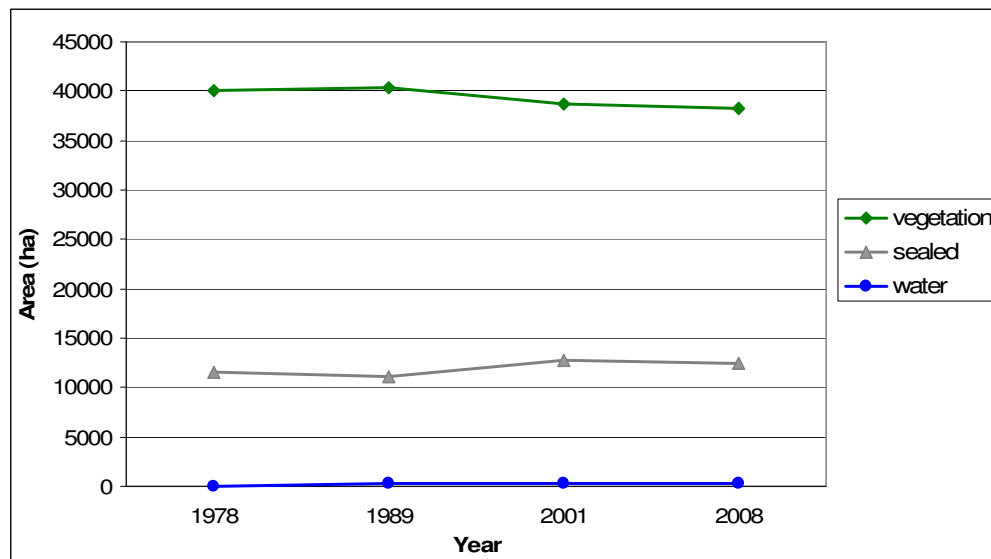


Figure 17. Temporal land-cover trends in the study area, derived from hard and soft classifications

Changes in sealed surface or vegetation cover can be visualised by subtracting the proportion maps of two dates cell-by-cell (e.g. map 2008 – map 1989). Although such maps may provide a quick view on temporal changes, the prediction errors present in each individual map introduce a certain level of noise in the vegetation or sealed surface proportion maps for each date. When these maps are subtracted from each other, the errors propagate. To deal with the uncertainty in proportion estimates, probability maps were produced indicating the likelihood a change of a certain magnitude occurs within a particular pixel. These probabilities were derived by placing an error distribution around the proportion differences for each pixel. We assume that the errors are normally distributed with a mean equal to $ME_{(t2-t1)}$ and standard deviation $\sigma_{(t2-t1)}$. The mean error of the difference map $ME_{(t2-t1)}$ could simply be calculated from:

$$ME_{(t2-t1)} = ME_{(t2)} - ME_{(t1)}$$

The error variance of the change map can be calculated from the error variances of two proportion maps as follows:

$$\sigma^2_{(t2-t1)} = \sigma^2_{(t1)} + \sigma^2_{(t2)} - 2COV_{(t1,t2)}$$

However, as errors can only be estimated for pixels for which vegetation proportions were calculated, the equation above can only be applied on pixels coinciding with the intersection of the urban areas defined by the hard classifications of $t1$ and $t2$. The probability calculations for the urban pixels of $t2$ that were not mapped as urban in $t1$ were determined directly from $\sigma_{(t2)}$ and $ME_{(t2)}$.

Using the calculated error variance and mean error, a normal probability density function can be centred on the calculated fraction difference obtained for each pixel to derive the chance that a change of a certain magnitude has occurred within that pixel (figure 18).

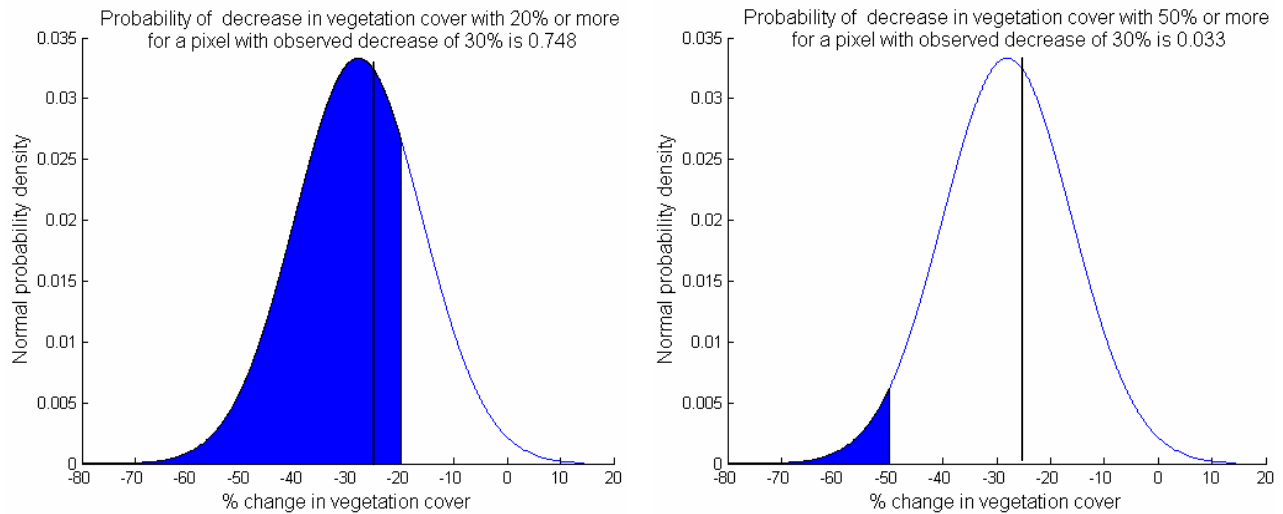


Figure 18. Calculation of change probabilities for 30% observed decrease in vegetation cover between 2008 and 1989

As an example, probability maps are shown indicating the chance that vegetation cover within a pixel has decreased with 20% or more between 1989 and 2008 (figure 19, left) and the chance of decreases with at least 50% (figure 19, right). These maps indicate areas where significant changes most likely occurred.

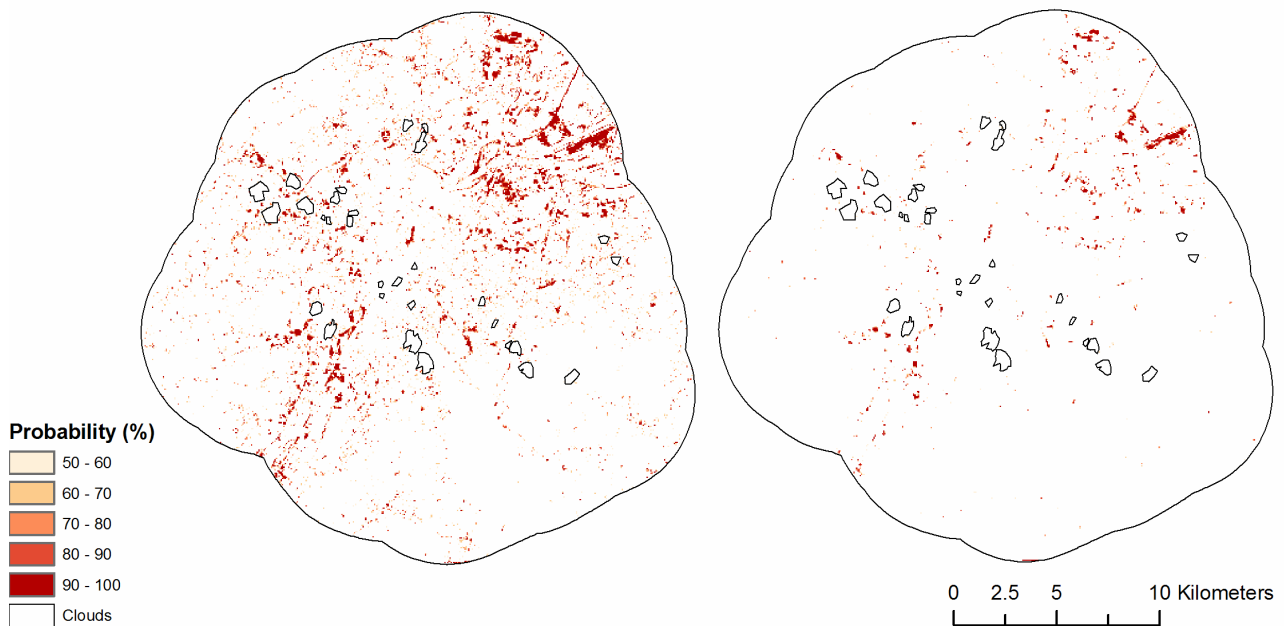


Figure 19. Change probabilities $\geq 50\%$ for decrease in vegetation cover between 2008 and 1989 $\geq 20\%$ (left) and $\geq 50\%$ (right)

Different types of urban growth emerge when we examine the maps in figure 19. We will not discuss all changes exhaustively, but highlight some manifest developments (figure 20). The largest change occurs at and near the international airport in Zaventem. This mostly involves an expansion of the tarmac and new airport buildings. Other clearly visible changes near the edge of the city and the ring road are mostly relatively large-scale industrial and commercial developments. Changes also occur within the

city itself, as the example of the new residential development at St. Lambrechts-Woluwe, near the E40, shows. New low density residential developments, which mainly occur in the urban fringe are not visible on the map highlighting decreases in vegetation cover with more than 50% (figure 19, right). This is logical for this type of developments as they usually include certain amounts of vegetation. The map which shows decreases with 20% or more (figure 19, left) better indicates these land use changes.

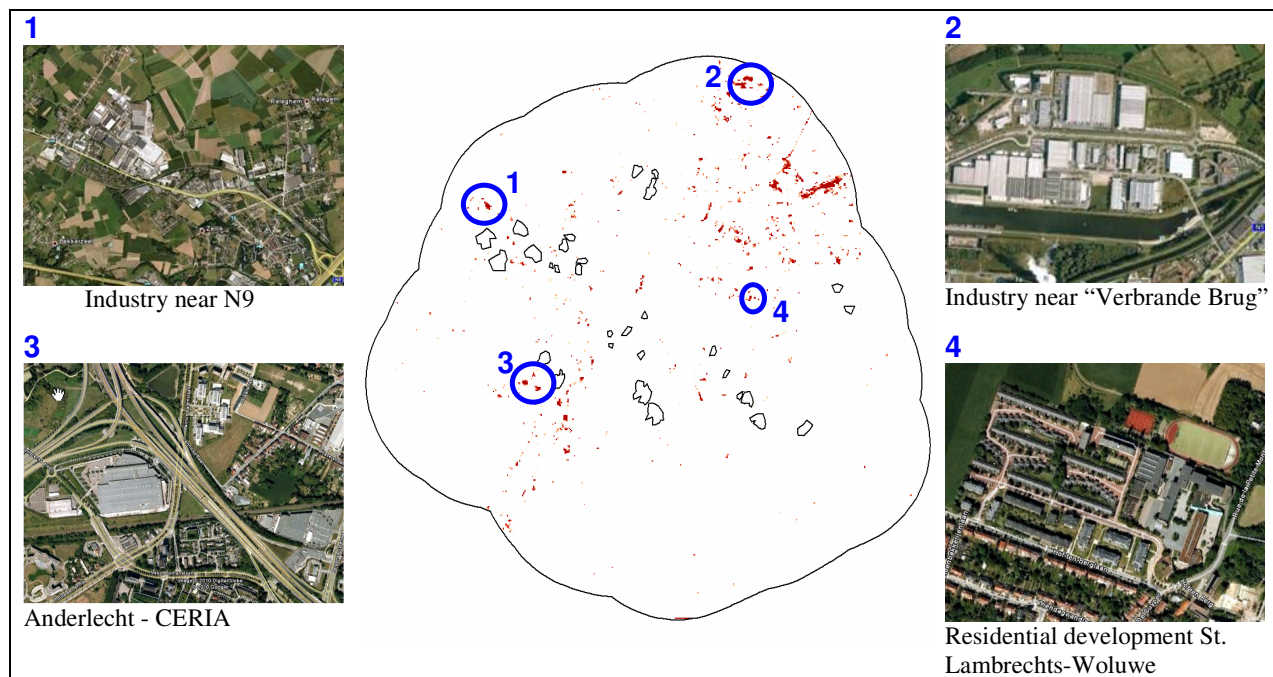


Figure 20. Some urban changes in Brussels between 1989 and 2008

4. Analysing temporal patterns of urban green with spatial metrics

Binary maps representing open and dense vegetation were derived from the “hard” land-cover maps (section 2) to serve as input for calculating spatial metrics with Fragstats. A minimum mapping unit of 3 and 5 ha was used for this purpose, which results in 4 maps for each image in the time-series. The same type of metrics as used in part I were produced for the study area defined for part II: number of patches and patch area statistics (table 11) and Euclidean nearest neighbour distance statistics (*ENN*) (table 12). In addition, patch density (*PD*) was calculated (table 11) to express the number of patches on a per unit area basis. *PD* is a landscape metric (i.e. one value is determined for the entire study area) and is calculated as follows:

$$PD = \frac{N}{A}(10000)(100)$$

where:

N = the total number of patches in the landscape (i.e. study area),

A = total area of the landscape in m².

Multiplication by 10 000 and 100 means that *PD* is expressed as number of patches per 100 hectares.

The patch size distribution of open vegetation is skewed in all years with a majority of small patches and fewer large patches. This is indicated by a median that is much smaller than the average (table 11): half of all patches of 3ha or more are smaller than about 6-7ha while the mean varies from 66ha in 1978 to 40ha in 2008. Open landscapes appear to become more fragmented through time as the number of patches increases and their average size becomes smaller. The decreasing standard deviation indicates that large patches become split up as time progresses. The steep drop between 2001 and 2008, for example, can be explained by a very large patch (6850ha) in the western part of the study area that splits up into several smaller patches (see also figure 13). Increasing fragmentation is mainly caused by new residential development in the urban fringe. However, the improved detection of linear features in the SPOT image due to its higher resolution (20m) is also partly responsible for the increase in number of patches between 2008 and the previous years. The same reasoning can be extended to a comparison between the 1988/2001 images and the 1978 image.

			NP	PD	AREA MN (ha)	AREA SD	AREA MD	AREA CV
Open vegetation	3ha	1978	230	0.321	65.7814	506.6833	7.200	770.2533
		1988	282	0.393	54.8295	439.5881	6.210	801.7369
		2001	279	0.388	52.7310	414.4602	6.210	785.9901
		2008	309	0.431	39.9508	184.3123	6.840	461.3482
	5ha	1978	156	0.217	95.1069	613.0548	11.700	644.5953
		1988	170	0.237	88.4711	563.6465	10.440	637.0971
		2001	165	0.230	86.5549	536.339	11.970	619.6518
		2008	204	0.285	58.5837	224.5757	11.300	383.3415
Dense vegetation	3ha	1978	280	0.390	39.8906	433.7409	6.120	1087.3270
		1988	240	0.334	39.0547	416.9044	5.760	1067.4869
		2001	246	0.342	34.1202	349.9684	5.805	1025.6914
		2008	202	0.282	36.4398	250.1473	5.820	686.4671
	5ha	1978	178	0.248	60.5083	542.9269	10.260	897.2766
		1988	152	0.212	59.4746	522.7794	8.460	878.9960
		2001	148	0.206	54.1277	450.0812	8.640	831.5173
		2008	121	0.169	58.3382	321.3499	11.040	550.8397

Table 11. Number of patches (*NP*), patch density (*PD*) and summary statistics for patch size: mean patch size (*AREA MN*), standard deviation (*AREA SD*), median (*AREA MD*) and coefficient of variation (*AREA CV*)

The average size of dense vegetation patches, on the contrary, does not change significantly with time. Their number, however, decreases, which also leads to a decreasing patch density in the study area. Most patches disappear west and northeast of the Sonian forest as they become smaller than the minimum mapping unit due to increasing fragmentation (figure 14). The decline in standard deviation is caused by the partitioning of a large contiguous patch consisting of the Sonian forest and surrounding forested areas. This patch measures 6478 ha in 1989, but decreases to 5505 ha in 2001 because parts near its edge are split into smaller patches as their connection to the main patch is severed. The further decrease of standard deviation in 2008 is caused by a division of the Sonian forest itself into three different patches because of a better detection of the roads running through the forest (R0 and E411). This is a consequence of increasing image resolution and has no ecological significance.

As was the case for the statistics in part I, a distance threshold has been applied for calculating *ENN* statistics to take into account that a relatively large part of the patches are in close proximity to each other. In this case, the threshold was set to 100m and patches that were closer to another patch of the same type were not considered as separate from an ecological point of view. Patches with an *ENN* distance smaller than 100m have therefore not been taken into account for calculating descriptive statistics of *ENN*. As a threshold of 100m corresponds to only 1.6 pixels in the 1978 image (1.18 if the diagonal is considered), no patches fall below the threshold in this image because a pixel distance of at least 2 is required for obtaining separate patches. For the other years, open vegetation clearly has a larger fraction of patches that are very close together than dense vegetation (table 12). This is the opposite of what was observed within the administrative bounds of the BCR in part I, which is no surprise given the fact that more open landscapes are present in the study area defined for part II, while the BCR itself is dominated by dense vegetation. For 1989, 62% of all open vegetation patches smaller than 3ha are located within 100m from another open vegetation patch. This fraction increases steadily to almost 70% for the year 2008. For the 5ha scenario, connectivity of open vegetation patches within a distance of 100m is somewhat higher than in the 3ha case (between 69% and 74%). Connectivity of dense vegetation patches is much less and decreases slightly in time for the 3ha as well as the 5ha scenario. This may be explained by the decreasing number of smaller patches.

			NP	NP <100m	NP ≥100m	% <100m	% ≥100m	ENN MN	ENN STD	ENN MD	ENN CV
Open vegetation	3ha	1979	230	0	230	0.00	100.00	236.52	276.06	134.16	116.72
		1989	282	176	106	62.41	37.59	318.99	366.73	169.71	114.96
		2001	279	183	96	65.59	34.41	343.08	389.88	184.87	113.64
		2008	309	214	95	69.26	30.74	254.88	217.78	215.41	85.44
	5ha	1979	156	0	156	0.00	100.00	214.98	269.29	134.16	125.26
		1989	170	117	53	68.82	31.18	263.21	378.66	150.00	143.86
		2001	165	117	48	70.91	29.09	290.06	394.83	174.85	136.12
		2008	204	151	53	74.02	25.98	223.14	141.91	156.21	63.60
Dense vegetation	3ha	1979	280	0	280	0.00	100.00	267.24	288.69	134.16	108.03
		1989	240	103	137	42.92	57.08	420.25	356.09	296.98	84.73
		2001	246	108	138	43.90	56.10	419.68	382.50	258.07	91.14
		2008	202	78	124	38.61	61.39	363.05	304.42	260.00	83.85
	5ha	1979	178	0	178	0.00	100.00	229.59	223.62	134.16	97.40
		1989	152	73	79	48.03	51.97	378.75	294.57	256.32	77.78
		2001	148	71	77	47.97	52.03	369.32	310.67	241.87	84.12
		2008	121	53	68	43.80	56.20	340.69	285.68	255.30	83.85

Table 12. Total number of patches (NP), number of patches less than 100m and more than 100m separated from a neighbouring patch (NP<100m, NP≥100m), and summary statistics for Euclidean nearest neighbour distance (ENN) for patches with ENN ≥ 100m : mean ENN (ENN MN), standard deviation (ENN SD), median (ENN MD) and coefficient of variation (ENN CV)

Summary statistics of *ENN* were calculated based on all patches that have no neighbour within 100m in order to examine patch isolation over larger distances. As was the case for patch area, *ENN* also produces a skewed distribution where patches that are close to a patch of the same type clearly dominate (figure 21). This indicates a tendency for spatial clustering of patches. In both the 3 and 5ha scenario, spatial clustering of dense vegetation patches is somewhat less pronounced as the mean distance between a patch and its closest neighbour is generally higher for dense vegetation. In 1978, the mean *ENN* for dense vegetation is only about 10% higher, but this is related to the low image resolution as the smallest patches may not be detected. For the other years, mean *ENN* for dense vegetation is 30-50% higher than for open vegetation, without big differences between the 3 and 5ha scenarios.

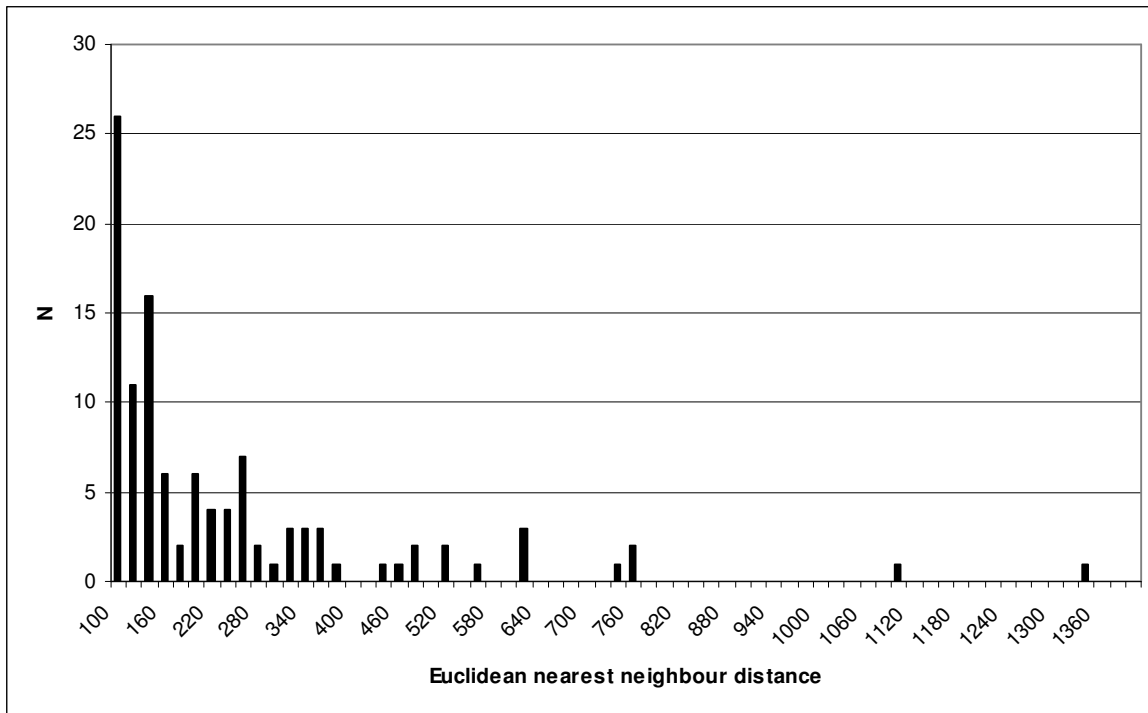


Figure 21 . Frequency distribution of Euclidean nearest neighbour distance for open vegetation patches (MMU 3ha) more than 100m separated from their closest neighbour

CONCLUSION

In this project, the use of high and medium resolution satellite data was examined for mapping urban green, for analysing spatial patterns of urban green and for monitoring changes of green cover through time. Recent high resolution imagery allowed us to develop detailed maps of open and dense vegetation within the administrative bounds of the Brussels Capital Region. These maps taught us that 54% of the Brussels Region was covered by vegetation at the moment of image acquisition (May/June 2008), with most green located near the city's periphery. Dense vegetation clearly dominated as it covered 44.25% of the region. Fragmentation of open vegetation was relatively high as it consisted of a large number of patches. Dense vegetation, by contrast, was less fragmented and patches of this type generally demonstrated a high degree of clustering. To study temporal changes in vegetation cover, medium resolution data had to be used. The study area for the temporal analysis was defined as the administrative region plus a buffer of 5km around it. Vegetation in this area consisted mostly of open vegetation as the rural surroundings of Brussels were also included. Two types of maps were derived for the four images constituting the time series: (hard) land-cover maps and (soft) proportion maps. The land-cover maps comprise four classes: open vegetation, dense vegetation, urban areas and water. They indicated that about 4500ha of land became urbanised during the time-period covered by the images. Image pixels in medium resolution data, however, often contain multiple land-cover types such as the mixed built-up/vegetation composition that is typical for low density residential areas. This led to an underestimation of actual vegetation cover in the hard land-cover maps. To take this into account, sub-pixel classification based on linear regression analysis was carried out to derive proportion maps of vegetation and sealed surface cover. These maps provided a more moderate view on the decline of vegetation cover (about 1900ha), but we should take into account that some of the vegetation cover indicated by these maps is not part of natural areas but of private residences. Open vegetation became more fragmented with time and small dense vegetation patches disappeared, often because their area fell below the minimum mapping units. While increasing fragmentation was responsible for a large part of the changes in the landscape pattern described by the metrics, differences in image resolution also exerted an influence as patches frequently became split up due to a better detection of line infrastructure in images that provide more spatial detail.

REFERENCES

Bauer, M.E., Loffelholz, B.C., Wilson, B., 2008. Estimating and mapping impervious surface area by regression analysis of Landsat imagery. In: Weng, Q. (Ed.), *Remote Sensing of Impervious Surfaces*. CRC Press Taylor & Francis Group, Boca Raton FL, 3 – 19.

Gustafson, E. J., and G. R. Parker. 1992. Relationships between landcover proportion and indices of landscape spatial pattern. *Landscape Ecology* 7:101-110.

Kettunen, M., A. Terry, G. Tucker and A. Jones. 2007. *Guidance on the maintenance of landscape features of major importance for wild flora and fauna - Guidance on the implementation of Article 3 of the Birds Directive (79/409/EEC) and Article 10 of the Habitats Directive (92/43/EEC)*. Institute for European Environmental Policy (IEEP), Brussels, 114 pp. & Annexes.
http://ec.europa.eu/environment/nature/ecosystems/docs/adaptation_fragmentation_guidelines.pdf

McGarigal, K., and B.J. Marks. 1995. *FRAGSTATS: spatial pattern analysis program for quantifying landscape structure*. Gen. Tech. Report PNW-GTR-351, USDA Forest Service, Pacific Northwest Research Station, Portland, OR.

Qi, J., Chehbouni, A., Huete, A., Kerr, Y. and S. Sorooshian. 1994. Modified soil adjusted vegetation index (MSAVI), *Remote Sensing of Environment*, 48: 119-126.

Sylwester, A. 2009. *Green Infrastructure – supporting connectivity, maintaining sustainability*. European Commission, DG Environment. <http://green-infrastructure-europe.org/>

Turner, M. G. 1989. Landscape ecology: the effect of pattern on process. *Ann. Rev. Ecol. Syst.* 20:171-197.

Turner, M. G. 1990. Spatial and temporal analysis of landscape patterns. *Landscape Ecol.* 4:21-30.

Van de Voorde, T., De Genst, W., and F. Canters, 2007. Improving pixel-based VHR land-cover classifications of urban areas with post-classification techniques. *Photogramm. Eng. Remote Sens.* 73, 1017 – 1027.

Van de Voorde, T., Vlaeminck, J. and F. Canters, F., 2008. Comparing Different Approaches for Mapping Urban Vegetation Cover from Landsat ETM+ Data: A Case Study on Brussels, *Sensors*, 8: 3880-3902

Van de Voorde, T., De Roeck, T., and F. Canters, 2009. A comparison of two spectral mixture modelling approaches for impervious surface mapping in urban areas. *Int. J. Remote Sens.* 30, 4785 – 4806.